RADIATION PATTERNS OF SEISMIC SURFACE WAVES FROM NUCLEAR EXPLOSIONS

by

Harold Henry Kehrer

B.S., Tufts University
(1968)

Submitted in Partial Fulfillment

of the Requirements for the

Degree of Master of

Science

at the

Massachusetts Institute of
Technology
September, 1969

Signature of Author.....
Department of Geology and Geophysics, July 18, 1969

Certified by. .....
Thesis Supervisor

Accepted by... .....
Chairman, Departmental Committee
on Graduate Students

RADIATION PATTERNS OF SEISMIC SURFACE WAVES FROM NUCLEAR EXPLOSIONS

BY

Harold Henry Kehrer

Submitted to the Department of Geology and Geophysics on July 18, 1969 in partial fulfillment of the requirement for the degree of Master of Science

ABSTRACT

The source mechanism of underground nuclear explosions is studied by considering a composite source. An orthogonal double-couple superimposed on an isotropic explosive source adequately accounts for the observed Love waves. The relative strength of the double-couple component and the azimuth of the fault plane at the source are determined for eleven explosions by fitting the Love over Rayleigh wave amplitude radiation pattern. The fault plane azimuths of explosions in the Pahute Mesa portion of the Nevada Test Site are similar to the orientations of the local faults. Explosions in Yucca Flat show a possible dependence on the Yucca Fault system and on joint trends in the surrounding bedrock. In gereral, the agreement appears more than coincidental and tends to support the hypothesis that regional strain is released by nuclear explosions. The relative strength of the double-couple depends upon rock type and shot depth.

Thesis Supervisor: M. Nafi Toksöz
Title: Associate Professor of Geophysics

TABLE OF CONTENTS

INTRODUCTION

During recent years, underground nuclear explosions have provided seismologists with a powerful tool for the study of crustal properties and seismic wave transmission. Such explosions offer the advantages of accurate knowledge of location and origin time. In addition theory predicts that the source mechanism of explosions should be much simpler than that of earthquakes, since at large distances an explosion can be represented as a spherically symmetrical point source. With this as a model one would expect to find P, SV, and Rayleigh waves in the records of these events, but no SH or Love waves. However, horizontally polarized shear waves were generated by most of the larger explosions. In the case of Hardhat (Toksöz, et al., 1965), the Love waves were considerably larger than the Rayleigh waves. It is evident then that the simple explosive point source model must be somehow modified to explain the generation of these horizontally polarized shear waves. Toksöz, et al. (1965) have considered and rejected several possible mechanisms. The possibility of conversion from P, SV, and Rayleigh waves can be eliminated due to the fact that Love waves are not observed from the collapses following explosions in which Love waves were observed. For the same reason, near-source irregularities have been ruled out since the propagation paths for explosion and collapse are

identical. The mechanism which has been suggested (Brune and Pomeroy, 1963; Toksöz, et al., 1965) for the generation of SH and Love waves is the release of tectonic strain by the explosions. Press and Archambeau (1962) have proposed three ways in which this strain release might occur:

1) The introduction of a sizeable cavity into a pre-stressed mechanism will release the strain energy stored in that volume.

2) Cracking of the surrounding rock should occur in preferred directions in order to minimize stress conditions.

3) Stress induced at the cavity wall could trigger a small earthquake.

Press and Archambeau (1962) concluded that mechanism (1) alone could not account for a significant amount of the seismic energy. However, in combination with (2), a large amount of elastic radiation could be produced. In the case of the explosions Haymaker and Shoal, sufficient energy could have been provided by such a combination, (Toksöz, et al., 1965). However, in the case of Hardhat, the seismic energy due to strain release was about 18 times greater than that available in the cavity and surrounding non-linear zone, (Toksöz, et al., 1965). It was concluded in this case (Brune and Pomeroy, 1963; Toksöz, et al., 1965) that the shock wave from the explosion triggered an earthquake.

The radiation patterns of seismic surface waves pro-

vides a convenient method for studying source mechanisms. This has been applied to nuclear explosions (Brune and Pomeroy, 1963; Toksöz, et al., 1965; Toksöz and Clermont, 1967) by considering the radiation patterns to be the result of strain released waves superimposed on the explosion generated waves. The simplest spatial configuration for such a composite source can be considered to be an orthogonal double-couple combined with an explosive point source. The orthogonal double-couple is probably the best representation for an earthquake source, and therefore such a model should adequately account for the seismic energy due to movement along joints or a generated earthquake. This procedure was successfully applied to the explosions Hardhat, Haymaker and Shoal by Toksöz, et al. (1965), and to Bilby by Toksöz and Clermont (1967). In this paper the method is continued to other explosions at the Nevada Test Site.

THEORY

Using the notation of Toksöz, et al. (1965), the expressions for the far-field ground displacements, due to an explosive point source at the surface, are in cylindrical coordinates:

$$\omega_e(\omega) = \frac{c_1}{(2\pi r)^{1/2}} \cdot \exp(-\gamma_R r)\, k_R^{1/2} \left(\frac{\dot{u}_o^*}{\omega_o}\right) A_R(\omega)\, T(\omega) \cdot \exp\left[i(\omega t - k_R r - \varphi_s + \tfrac{3\pi}{4})\right]$$

$$(1)\quad q_e(\omega) = \frac{c_1}{(2\pi r)^{1/2}} \cdot \exp(-\gamma_R r)\, k_R^{1/2} \left(\frac{\dot{u}_o}{\dot{w}_o}\right) A_R(\omega)\, T(\omega) \cdot \exp\left[i(\omega t - k_R r - \varphi_s - \tfrac{3\pi}{4})\right]$$

$$v_e(\omega) = 0$$

where w_e, q_e, and v_e are the vertical, radial, and tangential components of displacement, c_1 is a constant, γ_R is the Rayleigh wave attenuation coefficient, r is the radial distance from the epicenter, k_R is the wave number, $\dot{u}_o$ and $\dot{w}_o$ are components of partical velocity at the surface, A_R is the medium response for Rayleigh waves due to a vertical force, and $T(\omega)$ and $\varphi_s(\omega)$ are the amplitude and phase spectra of the source time function. The fact that the tangential component, v_e, is 0 indicates that no Love waves are to be expected from such a source.

The general form of the far-field Rayleigh and Love wave displacements due to an orthogonal double-couple is given by Ben-Menahem and Harkrider (1964) as:

$$(2)\quad U = |\underline{R}||\underline{n}| \frac{1}{(2\pi r)^{1/2}} \cdot \exp\left[i(\omega t - k_h r - \tfrac{3\pi}{4})\right] k_h\, N(h)\, \chi(\theta)$$

where $\underline{R}$ is the displacement vector at the source, $\underline{n}$ is the normal vector to the plane of motion, k_h is either k_R or k_L, the Rayleigh and Love wave numbers, $N(h)$ is either $N_\theta(h)$ or $N_{r_2}(h)$, the Love wave singlet transfer function and the Rayleigh Wave second singlet transfer function, h is the source depth, and $\chi(\theta)$ is the complex function:

$$\chi(\theta) = d_0 + i(d_1 \sin\theta + d_2 \cos\theta) + d_3 \sin 2\theta + d_4 \cos 2\theta$$

where θ is the epicenter to station azimuth, measured counter-clockwise from the positive strike direction. For

a surface source d_1 and d_2 are 0 for both Love and Rayleigh waves, and $\chi(\theta)$ becomes:

$$\chi(\theta) = \tfrac{1}{2} \sin\lambda \sin 2\delta \sin 2\theta + \cos\lambda \sin\delta \cos 2\theta$$

for the tangential component; and

$$\chi(\theta) = \tfrac{1}{2} \sin\lambda \sin 2\delta \cdot \epsilon_0 \left(\frac{1+\sigma_0}{1-\sigma_0}\right) + \epsilon_0 \cos\lambda \sin\delta \sin 2\theta - \tfrac{1}{2} \epsilon_0 \sin\lambda \sin 2\delta \cos 2\theta$$

for the radial component. δ and λ are the dip and slip direction respectively, ϵ_0 is ellipicity, and σ_0 is Poisson's ratio at the surface. Thus the far field displacements will depend on the source parameters, δ and λ, and the azimuth θ. These displacements become:

$$v_{dc}(\omega) = |\underline{R}||\underline{n}| \frac{1}{(2\pi r)^{1/2}} \cdot \exp\left[i(\omega t - k_L r - \tfrac{3\pi}{4})\right] k_L N_\theta(0) \cdot \left[\tfrac{1}{2} \sin\lambda \sin 2\delta \sin 2\theta + \cos\lambda \sin\delta \cos 2\theta\right]$$

$$(3)\quad q_{dc}(\omega) = |\underline{R}||\underline{n}| \frac{1}{(2\pi r)^{1/2}} \cdot \exp\left[i(\omega t + k_R r - \tfrac{3\pi}{4})\right] k_R N_{rz}(0) \epsilon_0 \cdot \left[\tfrac{1}{2} \sin\lambda \sin 2\delta \left(\frac{1+\sigma_0}{1-\sigma_0} - \cos 2\theta\right) + \cos\lambda \sin\delta \sin 2\theta\right]$$

$$\omega v_{dc}(\omega) = q_{dc}(\omega) / \epsilon_0 \exp(i\tfrac{\pi}{2})$$

$$= |\underline{R}||\underline{n}| \frac{1}{(2\pi r)^{1/2}} \cdot \exp\left[i\omega t - k_R r + \tfrac{2\pi}{4}\right] k_R N_{rz}(0) \cdot \left[\tfrac{1}{2} \sin\lambda \sin 2\delta \left(\frac{1+\sigma_0}{1-\sigma_0} - \cos 2\theta\right) + \cos\lambda \sin\delta \sin 2\theta\right]$$

The medium transfer functions can be expressed (Ben-Menahem and Harkrider, 1964) in terms of particle velocities as:

$$N_\theta(h) = \left[\dot{v}_s(h) / \dot{v}_0\right] A_L(\omega) k_L^{-1/2}$$

$$N_{rz}(h) = -\left[\dot{u}_s^*(h) / \dot{v}_0\right] A_R(\omega) k_R^{-1/2}$$

where $\dot{u}_s^*(h) = -i\,\dot{u}_s(h)$; $\dot{u}_0(h)$, $\dot{v}_0(h)$, $\dot{w}_0(h)$ are particle velocities at the surface. A_R and A_L are the Rayleigh and Love amplitude factors, which are functions of the medium.

For a surface source, $h=0$ and the transfer functions become:

$$N_\theta(0) = A_L(\omega)\, k_L^{-1/2}$$

$$N_{zr}(0) = N_{rz}(0)$$

$$N_{rz}(0) = -\left[\dot{u}_0^* / \omega_0\right] A_R(\omega)\, k_R^{-1/2}$$

$$\epsilon_0\, N_{rz}(0) = -\left[\dot{u}_0^* / \omega_0\right] N_{rz}(0)$$

$$= \left[\dot{u}_0^* / \omega_0\right]^2 A_R(\omega)\, k_R^{-1/2}$$

After substituting these relations, the far-field displacements due to the double-couple at the surface are:

$$w_{dc}(\omega) = \frac{|R||n|}{(2\pi r)^{1/2}} \cdot \exp\left[i(\omega t - k_R r - \varphi_c' + \tfrac{3\pi}{4})\right] k_R^{1/2} \left(\frac{\dot{u}_0^*}{\omega_0}\right) A_R(\omega)\, T'(\omega) \exp(-\delta_R r) \cdot$$
$$\left[\tfrac{1}{2} \sin\lambda \sin 2\delta \left(\frac{1+\epsilon_0}{1-\epsilon_0} - \cos 2\theta\right) + \cos\lambda \sin\delta \sin 2\theta\right]$$

$$(4)\quad q_{dc}(\omega) = \frac{|R||n|}{(2\pi r)^{1/2}} \cdot \exp\left[i(\omega t - k_R r - \varphi_c' - \tfrac{3\pi}{4})\right] k_R^{1/2} \left(\frac{\dot{u}_0^*}{\omega_0}\right)^2 A_R(\omega)\, T'(\omega) \exp(-\delta_R r) \cdot$$
$$\left[\tfrac{1}{2} \sin\lambda \sin 2\delta \left(\frac{1+\epsilon_0}{1-\epsilon_0} - \cos 2\theta\right) + \cos\lambda \sin\delta \sin 2\theta\right]$$

$$v_{dc}(\omega) = \frac{|R||n|}{(2\pi r)^{1/2}} \cdot \exp\left[i(\omega t - k_L r - \varphi_c' - \tfrac{3\pi}{4})\right] k_L^{1/2} A_L(\omega)\, T'(\omega) \exp(-\delta_L r) \cdot$$
$$\left[\tfrac{1}{2} \sin\lambda \sin 2\delta \sin 2\theta + \cos\lambda \sin\delta \cos 2\theta\right]$$

Considering the observed displacements to be due to the combination of isotropic and double-couple sources, the Rayleigh and Love wave displacements can be written in the notation of Toksoz, et al. (1965) as:

$$U_{RZ}(\omega) = \omega_e(\omega) + \omega_{dc}(\omega)$$

$$= \omega_e(\omega) \left\{ 1 + F \frac{T'(\omega)}{T(\omega)} e^{i\delta\varphi} \cdot \right.$$

(5)

$$\left. \left[\tfrac{1}{2} \sin\lambda \sin 2\delta \left(\frac{1+\epsilon_0}{1-\epsilon_0} - \cos 2\theta \right) + \cos\lambda \sin\delta \sin 2\theta \right] \right\}$$

$$U_{L\theta}(\omega) = \omega_{dc}(\omega)$$

where $\delta\varphi$ is the phase difference between the two time functions, and the constant F is the strength of the double-couple source, relative to that of the explosion. If the difference between time functions $T(\omega)$ and $T'(\omega)$ is considered negligible (Toksöz, et al., 1965), the displacements become:

$$U_{RZ} = \omega_e \left\{ 1 + F \left[\tfrac{1}{2} \sin\lambda \sin 2\delta \left(\frac{1+\epsilon_0}{1-\epsilon_0} - \cos 2\theta \right) + \cos\lambda \sin\delta \sin 2\theta \right] \right\}$$

(6)

$$U_{L\theta} = \omega_{dc}$$

Theoretically, if the properties of the medium of propagation are known, the source function can be determined from seismic records. However, these properties are rarely, if ever known. Thus any computed source function must be an approximation only. In addition surface waves radiating from a source are modified by attenuation, dispersion, geometrical spreading, and instrument response. These effects can be removed by phase or amplitude equalization. It is possible to remove these effects and those of the propagation path by some sort of normalization. If attenuation of Rayleigh and Love waves is assumed to be about the same, the ratio of the observed Love wave ampli-

tude to that of the vertical component of the Rayleigh wave can be determined:

$$(7)\quad \frac{|u_{L0}|}{|u_{R2}|} = \frac{F k_L^{1/2} A_L \left[\tfrac{1}{2} \sin\lambda \sin 2\delta \sin 2\theta + \cos\lambda \sin\delta \cos 2\theta \right]}{\left\{ 1 + F \left[\tfrac{1}{2} \sin\lambda \sin 2\delta \left(\frac{1+\epsilon_0}{1-\epsilon_0} - \cos 2\theta \right) + \cos\lambda \sin\delta \sin 2\theta \right] \right\} k_R^{1/2} A_R \left(\frac{\dot{u}_0^*}{\omega_0} \right)}$$

For a horizontal double-couple $\lambda = 0^\circ$ and $\delta = 90^\circ$, and equation (7) simplifies to:

$$(8)\quad \frac{|u_{L0}|}{|u_{R2}|} = \frac{F k_L^{1/2} A_L \cos 2\theta}{\left\{ 1 + F \sin 2\theta \right\} k_R^{1/2} A_R \left(\frac{\dot{u}_0^*}{\omega_0} \right)}$$

DATA

In this paper Love over Rayleigh wave amplitude ratios are computed at stations recording surface waves from several Nevada Test Site explosions. The best fit of this data to the above equation (8) is then determined and the source parameters are obtained.

Eleven recent nuclear explosions were analysed. Information regarding these is given in Table 1. Love and Rayleigh wave amplitudes were obtained from the long period records of Long Range Seismic Measurements (LRSM) stations, World Wide Standard Systems (WWSS) stations. and some stations of the Canadian network. The stations were located in North and Central America, particularly in the United States. The response of nearly all the instruments peaked at about 25 seconds period. Sample seismograms of the explosion Greeley are reproduced in Figures 1-3. The recording station is Resolute Bay in northwestern Canada,

about 4,300 km from the Nevada Test Site. Rayleigh waves are recorded on the vertical component and Love waves on the east-west component. Both appear clearly separated on the north-south component.

At the LRSM stations, amplitudes of Love and vertical component Rayleigh waves were taken from the reports prepared for AFTAC by Teledyne Industries, Inc. At the WWSS and Canadian stations, amplitudes were measured directly from the film records. In all cases peak amplitudes were taken and used in computing the amplitude ratios. This was shown by Toksöz and Clermont (1967) to be justifiable, since the ratio is nearly constant in the period range of 10 to 30 seconds. At each station, the peak amplitudes of Love and Rayleigh waves were divided by the period and instrument response. The Love over Rayleigh wave ratio of these measurements was then computed. Unfortunately the azimuthal distribution of recording stations with respect to the Nevada Test Site is not uniform. Between 160 and 330 degrees, there is little or no coverage depending upon the explosion. In addition, inconsistencies due to measurement errors occur along a single azimuth. It is obvious, however, that the ratio is not constant.

From equation (7), it can be seen that the amplitude ratio is a function of four source parameters: F, the part double-couple, θ, the azimuth from the fault plane, δ, the

dip of the fault plane, and λ, the direction of slip. If a vertical strike-slip fault is assumed ($\delta = 90$ and $\lambda = 0$), then equation (7) reduces to equation (8). This is a reasonable assumption for such a near-surface source. The quantity $k_L^{1/2} A_L / k_R^{1/2} A_R$ is approximately equal to 1 in the frequency range of interest (Toksöz and Clermont, 1967). The ellipticity term $\dot{u}_o^* / \dot{w}_o$ is strongly influenced by near-surface sedimentary layers (Boore and Toksöz, 1969) and therefore varies with station location. However, to simplify calculations, an average value of .8 was taken for the ellipticity at each station. The effect of varying this term will be investigated later. The angle θ can be expressed as the difference between the fault plane azimuth Ψ and the station azimuth φ, both measured clockwise from the north:

$$\theta = \Psi - \varphi$$

Thus equation (8) becomes:

$$(9) \qquad \frac{|u_{L0}|}{|u_{R2}|} = S \left\{ \frac{F \cos 2(\Psi - \varphi)}{1 + F \sin 2(\Psi - \varphi)} \right\}$$

where S is a constant.

To determine F and Ψ, a "standard deviation" was formed between the data and all combinations of F from 0 to 2.0 and of Ψ from 0 to 180 degrees:

$$(10) \qquad E_j = \sum_{i=1}^{N} \sqrt{\left(L_i/R_i - \left| \frac{S \cdot F_j \cos 2(\Psi_j - \varphi_i)}{1 + F_j \sin 2(\Psi_j - \varphi_i)} \right| \right)^2 / N}$$

The combination of F and Ψ which fits the data best, will

be that which minimizes E. Here L/R is the experimentally measured Love over Rayleigh wave amplitude ratio, and N is the number of stations. The values of E were then contoured on a Stromberg Carlson-4020 grid to determine which combination of F and Ψ gave the best fit to the data. The result for the explosion Corduroy is presented in Figure 4. S was taken to be 1.25 (ellipticity of .8). The absolute minimum deviation was found to be .59, and it occured for a F=.6 double-couple source, with a right-lateral fault plane striking about 165 degrees from the north. The minimum is fairly well defined, but the deviation is high. This is probably due to the inconsistencies and bad points in the data.

To eliminate such inconsistencies, the data was first smoothed before attempting to fit the theoretical radiation pattern. The effect of a single data point was considered to be distributed over a "smoothing interval" of several degrees. New data was then generated at equal increments of azimuth. Where isolated points occur, the value is spread over the whole "smoothing interval." Where more points occur within the "smoothing interval," the influence of a single data point varies inversely as the distance from it, with the point at the center heavily weighted (should an actual data point fall on a generated azimuth value). The effect of a single data point was taken to extend 5 degrees in either direction, so that the "smooth-

ing interval" was 10 degrees.

The deviations of the smoothed data from theoretical source configurations were then contoured on a SC-4020 grid, as was done with the unsmoothed data. The results are shown in Figures 5-15 for the eleven explosions. The minima indicate the best combination of part double-couple and azimuth of a right lateral fault plane. A comparison of the contour plot for Corduroy, Figure 7, with that of the unsmoothed case, Figure 4, shows that the minimum deviation has been significantly reduced by the smoothing, although it is still rather high. Clear minima are observed in the plots for each explosion. However, secondary minima are also observed for most cases. This is most likely due to the fact that the theoretical curve is nearly periodic in 90 degrees. If it were truly periodic every 90 degrees, as are the individual radiation patterns of Love and Rayleigh waves, two minima would be observed in the 180 degree range, separated by 90 degrees. If the source model is accurate, then the data should exhibit this near periodicity in 90 degrees. Therefore double-minima are likely to occur. If the difference between the absolute and secondary minimum is not significant, then it is impossible to make a confident choice between the two configurations by this analysis. This is in addition to the basic theoretical ambiguity that the L/R radiation pattern for a right-lateral fault is the same as that for a left-lateral fault

with a difference in strike of 90 degrees, as is illustrated in Figure 16. This latter ambiguity can be resolved by other methods, such as utilizing phase information. A summary of Figures 5-15 is given in Table 2. The greater the difference between minima, the greater will be the certainty that the absolute minimum corresponds to the true solution for a particular explosion. Values for the minima are higher for explosions with a larger part double-couple. This is to be expected and does not imply that the results are less significant, since the term in absolute value in equation (10) becomes small for these explosions.

If the absolute minimum is assumed to correspond to the correct combination of source parameters, with the reservation that there may be other solutions, the theoretical radiation patterns can be compared to the experimental (unsmoothed) data. This is shown in polar coordinates in Figures 17-27 for the eleven explosions studied. Here the scatter in the data is very much apparent. A large part of this is probably due to errors in measurement, particularly of period. In any case, the convergence to minima in the contour plots indicates that the solutions are significant.

In fitting the theoretical curves, a vertical strike-slip fault at the source was assumed. To test this initial assumption, the best fitting values of F and θ for each explosion were substituted into equation (7). ϵ was taken

to be .25. The parameters δ and λ were then allowed to vary, and the deviations of the smoothed data were contoured for the various combinations. For all the explosions the minimum was found to be broad, but centered on $\delta = 90$ and $\lambda = 0$ degrees. Thus the initial assumption is reasonable. The fact that the contours are broad indicates that the radiation pattern is not as sensitive to variations in dip and slip than to variations in part double-couple and fault plane azimuth.

The effect of varying the scale factor S, which depends upon the medium of propagation, was next investigated. Values for S of .5, 1.0, 1.5, and 2.0 were substituted into equation (9). If the term $k_L^{1/2}A_L/k_R^{1/2}A_R$ remains equal to 1, these numbers correspond to ellipticities ($\dot{u}_o/\dot{w}_o$) of 2.0, 1.0, .67, and .5 respectively. Contour plots of F versus Ψ, the fault plane azimuth measured from the north, for each S were then obtained by the methods previously described. The results for the explosion Corduroy are shown in Figures 28-31. A comparison of these and Figure 7, where S=1.25, reveals that an increase in S causes a decrease in F, the part double-couple. The azimuth of the fault plane, however, remains invariant. Only for the extreme case where S=.5 is the absolute minimum shifted from the 166 degree position.

INTERPRETATION

If the hypothesis is correct that a part of the observed seismic radiation from a nuclear explosion is due to a double-couple source, then the orientation of the fault at the focus should be intimately related to the structure of the area. If stress is released, faulting should occur in preferred directions.

Structure of the Nevada Test Site Area

The Nevada Test Site covers an area of about 700 square miles in southern Nevada. About a third of the outcrops consists of Paleozoic and Precambrian sedimentary rocks, and another third consists primarily of volcanics and related intrusives of Tertiary age. The remainder of the area is covered by alluvium (Ekren, 1968). The southern part may possibly overlap the Walker Lane-Las Vegas Valley strike-slip shear zone. Two major thrust fault systems of Mesozoic age are found in the area. Faults in the northern part strike northward and appear to be primarily normal faults. Normal faulting began in the early Tertiary Age and has continued to recent time (Johnson and Hibbard, 1957). As the Las Vegas Valley shear zone is approached, the strike changes to northeast. Left-lateral movement is observed on several of these faults and may be the result of right-lateral slippage along the Las Vegas Valley shear zone. This zone was active at the time of the

main orogeny in Mesozoic time. However, it appears probable that activity continued through much of Tertiary time (Longwell, 1960). Thus the NTS area is a tectonically active region, and there is good reason to believe a sizeable amount of strain energy is stored in the ground.

Several of the explosions studied occurred in the Yucca Flat portion of the test site. This alluvium filled valley overlies and is surrounded by Tertiary volcanic rock. It is bordered by a series of normal faults and is nearly bisected lengthwise by the Yucca Fault of recent age. Explosions in Yucca Flat, particularly those in the tuff beneath the alluvium, produced fractures in the alluvium around the explosion site. These fractures occur not only in radial and concentric patterns, but are commonly alligned in certain preferential directions, which can be divided into two groups. The first group are those cracks that occur along and parallel to the Yucca Fault, and the second, those whose direction is controlled by joints in the underlying bedrock (Barosh, 1968; Dickey, 1968). Observed displacements are usually normal.

Fault Plane Solutions in Relation to Structure

Figure 32 is a generalized geologic map of the NTS and shows the explosions studied (numbers refer to Table 2) in relation to the major faults in the area. The explosion Faultless did not occur at the NTS and therefore does not

appear on the map. The fault plane solutions for each explosion of Table 2 can now be compared to the natural fracture patterns. The explosions which follow occurred in Yucca Flat.

1. Cup: For Cup, a right-lateral fault plane with an azimuth of about 112 degrees (or a left-lateral fault at 22 degrees), gives the best fit to the data. The other possible orientation, azimuth 2 of Table 2, is the same except that the sense of the couple is reversed. Figure 33 shows the best orientation of the double-couple in relation to both the natural fracture trends and those produced in the alluvium by explosions. The agreement is not very good, although there is a weak north-northeast trend present in the alluvium and in certain places in the bedrock of Banded Mountain.

2. Bronze: Two fault plane solutions are equally likely for Bronze, Table 2. They are close, however, except that the sense of the couple is reversed. The solution with the right-lateral fault at an azimuth of 94 degrees is shown in Figure 33. Again the agreement with explosion produced fractures in the alluvium is not good. However, the dominant trend in the bedrock on the east side of Slanted Buttes (not shown in Figure 33) nearby is north-northeast, as is the fault plane.

3. Corduroy: The azimuth of the best fitting right-lateral fault plane for Corduroy is 166 degrees. The second

solution is again close to this except that the sense of the faults is reversed. Numerous en echelon fractures along the Yucca Fault were produced in the alluvium by Corduroy (Barosh, 1968). Such an en echelon pattern is generally related to major strike-slip movement in the underlying basement (Badgley, 1965). The trend of the pattern in this case suggests right-lateral slippage. Thus the solution of a right-lateral fault with strike of 166 degrees, which is similar to that of the Yucca Fault, is in good agreement with the local trends.

4. Buff: The best solution for Buff is that of a right-lateral fault at 28 degrees (left-lateral fault at 118 degrees). The second solution is close to this but reversed in sense.

5. Tan: The two solutions for Tan are essentially equally probable. The solution of a right-lateral fault at 26 degrees is similar to that obtained for Buff, only .75 km away. However, the azimuth of 154 degrees is close to that obtained for Bilby (160 degrees, Toksöz and Clermont, 1967) about 1.45 km away.

The other explosions studied (excluding Faultless) occurred in the Pahute Mesa portion of the NTS. The main structural feature of Pahute Mesa is the Silent Canyon Caldera, which encloses the five explosions studied. Many normal faults, striking north-northeast, cut the thick sequence of volcanic rock. Recent movement along some of

these faults has been inferred (McKeown, et al., 1966).

Reference to Table 2 reveals that the best fitting fault plane azimuth for the five explosions, numbered 5, 6, 8, 9, and 11, range from 160 to 180 degrees. These orientations are in close agreement with the regional fault trends.

The relative strength F of the double-couple ranged from .36 to .9 for the explosions studied. The dependence of this parameter on lithology has been noted (Toksöz, 1967). Explosions in granite have a larger double-couple component than those in tuff, which in turn have a larger component than those in alluvium. This supports the hypothesis of strain release since granite can sustain greater strain energy than tuff, and tuff greater than alluvium. From this study it is concluded that F also depends upon the shot depth. Deeper shots have a larger double-couple component than shallow shots. The principal deviations from this F - depth relation are due to lithology. The deep explosion Faultless had a smaller double-couple component than expected due to the water-saturated medium. The low double-couple part of .45 for Boxcar, however, can not be explained.

CONCLUSIONS

Love waves produced by all the explosions studied, can be accounted for by considering the source to be a superposition of symmetrical explosion and tectonic double-

couple components. The fault plane solutions appear to be consistent with the hypothesis that regional strain is released. Inferred orientations for the explosions in Pahute Mesa show good agreement with the local fault trends. Some of the explosions on Yucca Flat appear related to the Yucca Fault system, while others may be controlled by joint trends in the underlying bedrock. The strength of the double-couple component, for a particular explosion, depends upon the shot depth as well as the rock type. Aki, et al. (1969) have shown that the probable strain release from a nuclear explosion is characteristic of a low efficiency, less dangerous earthquake. Thus the definite possibility exists of safely releasing strain in tectonically active areas.

ACKNOWLEDGEMENTS

The writer is indebted to Prof. M. Nafi Toksöz of Massachusetts Institute of Technology for suggesting the topic and porviding advice through the course of the work. Thanks are also extended to Mr. Ron Ward of M.I.T. for providing the SC-4020 contouring routine as well as valuable discussions. This work was supported by the United States Air Force Office of Aerospace Research and monitored by Air Force Cambridge Research Laboratories under Contract No. F 19628-68-C-0043.

REFERENCES

Aki K., p. Reasenberg, T. DeFazio and Y. Tsai (1969). Near-field and Far-Field Seismic Evidences for Triggering of an Earthquake by the Benham Explosion, paper presented at the annual meeting of the AGU, April, 1969.

Badgley, P. C. (1965). Structural and Tectonic Principles, Harper and Row, N.Y.

Barosh, P. J. (1968). Relationship of Explosion-produced Fracture Patterns to Geologic Structure in Yucca Flat, Nevada Test Site, Geol. Soc. Am. Mem. 110, Nevada Test Site, 199-217.

Ben-Menahem, A. and D. G. Harkrider (1964). Radiation Patterns of Seismic Surface Waves From Buried Dipolar Point Sources in a Flat Stratified Earth, J. Geophys. Res. 69, 2605-2620.

Boore, D. M. and M. N. Toksöz (1969). Rayleigh Wave Particle Motion and Crustal Structure, Bull. Seism. Soc. Am. 59, 331-346.

Brune, J. N. and P. W. Pomeroy (1963). Surface Wave Radiation Patterns for Underground Nuclear Explosions and Small-magnitude Earthquakes, J. Geophys. Res. 68, 5005-5028.

Dickey, D. D. (1968). Fault Displacement as a Result of Underground Nuclear Explosions, Geol. Soc. Am. Mem. 110, Nevada Test Site, 219-232.

Ekren, E. B. (1968). Geologic Setting of Nevada Test Site and Nellis Air Force Range, Geol. Soc. Am. Mem. 110, Nevada Test Site, 11-19.

Healey, D. L. (1968). Application of Gravity Data to Geologic Problems at Nevada Test Site, Geol. Soc. Am. Mem 110, Nevada Test Site, 147-156.

Hoover, D. L. (1968). Genesis of Zeolites, Nevada Test Site, Geol. Soc. Am. Mem. 110, Nevada Test Site, 275-284.

Johnson, M. S. and D. E. Hibbard (1957). Geology of the Atomic Energy Commission Nevada Proving Grounds Area, Nevada, USGS Bull. 1021-K, 333-384.

Longwell, C. R. (1960). Possible Explanation of Diverse Structural Patterns in Southern Nevada, Am. Jour. Sci, 258-A (Bradley Volume), 192-203.

McKeown, F. A., P. P. Orkild, D. D. Dickey and R. P. Snyder (1966). Some Geologic Data Pertinent to the Seismic Characteristics of Pahute Mesa, USGS Tech-letter: Sp. Std. I-45.

Press, F. and C. Archambeau (1962). Release of Tectonic Strain by Underground Nuclear Explosions, J. Geophys. Res. 67, 337-343.

Teledyne Industries, Inc., Earth Sciences Division (1965). Long Range Seismic Measurements - Bronze, Seismic Data Lab. Report No. 132.

Teledyne Ind. Inc., Earth Sci. Div. (1966). LRSM - Cup, SDL Report No. 136.

Teledyne Ind. Inc., Earth Sci. Div. (1966). LRSM - Buff, SDL Report No. 143.

Teledyne Ind. Inc., Earth Sci. Div. (1966). LRSM - Duryea, SDL Report No. 153.

Teledyne Ind. Inc., Earth Sci. Div. (1966). LRSM - Corduroy, Geotech. Tech. Report No. 66-43.

Teledyne Ind. Inc., Earth Sci. Div. (1966). LRSM - Tan, SDL Report No. 169.

Teledyne Ind. Inc., Earth Sci. Div. (1967). LRSM - Greeley, SDL Report No. 180.

Teledyne Ind. Inc., Earth Sci. Div. (1968). LRSM - Faultless, SDL Report No. 215.

Teledyne Ind. Inc., Earth Sci. Div. (1968). LRSM - Boxcar, SDL Report No. 223.

Teledyne Ind. Inc., Earth Sci. Div. (1966). LRSM - Half Beak, SDL Report No. 171.

Toksöz, M. N. (1967). Radiation of Seismic Surface Waves from Underground Explosions, Proceedings of the VESIAC Conference on the Current Status and Future Prognosis for Understanding the Source Mechanism of Shallow Seismic Events in the 3 to 5 Magnitude Range, Report of VESIAC 7885-1-X, Willow Run Laboratories, 65-83.

Toksöz, M. N. and K. Clermont (1967). Radiation of Seismic Waves from the Bilby Explosion, SDL Report No. 183.

Toksöz, M. N., D. G. Harkrider and A. Ben-Menahem (1965). Determination of Source Parameters by Amplitude Equalization of Seismic Surface Waves 2. Release of Tectonic Strain by Underground Nuclear Explosions and Mechanism of Earthquakes, J. Geophys. Res. 70, 907-922.

Table 1. EXPLOSION INFORMATION

EVENT	DATE	ORIGIN TIME GMT	LOCATION N. LAT.	W. LONG.
1. Cup	3-26-65	15:34:08.2	37°08'51"	116°02'34"
2. Bronze	7-23-65	17:00:00.0	37°05'52"	116°01'59"
3. Corduroy	12-03-65	15:13:02.1	37°09'53"	116°03'08"
4. Buff	12-16-65	19:15:00.0	37°04'21"	116°01'45"
5. Duryea	4-14-66	14:13:43.1	37°14'34"	116°25'51"
6. Chartreuse	5-06-66	15:00:00.1	37°20'53"	116°14'19"
7. Tan	6-03-66	14:00:00.0	37°04'06"	116°02'07"
8. Half Beak	6-30-66	22:15:00.1	37°18'57"	116°17'56"
9. Greeley	12-20-66	15:30:00.1	37°18'07"	116°24'30"
10. Faultless	1-19-68	18:15:00.1	38°38'03"	116°12'55"
11. Boxcar	4-26-68	15:00:00.0	37°17'44"	116°27'21"

Table 2. FAULT PLANE SOLUTIONS

EVENT	EQUIV. MAG.	DEPTH ft	MEDIUM	MIN. DEV. FROM DATA	PART DOUBLE-COUPLE	RT.-LA AZIMU
1. Cup	5.25	2470	Tuff	.50	.60	11
2. Bronze	5.22	1750	Tuff	.20	.36	1
3. Corduroy	5.62	2248	Tuff	.44	.60	16
4. Buff	5.14	1650	Tuff	.20	.38	2
5. Duryea	5.17	1795	Rhyolite	.33	.56	16
6. Chartreuse	5.2	-	Rhyolite	.33	.63	17
7. Tan	5.56	1840	Tuff	.23	.36	15
8. Half Beak	6.02	2884	Rhyolite	.56	.57	16
9. Greeley	6.29	4040	Zeolitized Tuff	1.31	.90	18
10. Faultless	6.25	3200	Water Saturated Tuff	.16	.36	10
11. Boxcar	6.14	3800	Rhyolite	.28	.45	16

FIGURE CAPTIONS

Fig. 1. Rayleigh waves from the Greeley explosion on long-period vertical component at Resolute Bay, Canada.

Fig. 2. Love and Rayleigh waves from the Greeley explosion on long-period north-south component at Resolute Bay, Canada.

Fig. 3. Love waves from the Greeley explosion on long-period east-west component at Resolute Bay, Canada.

Fig. 4. Contour plot of deviations of combinations of part double-couple and fault plane azimuth from experimental data for the explosion Corduroy. Experimental data not smoothed. Scale factor, S=1.25.

Figs. 5 - 15. Contour plots of deviations of combinations of part double-couple and fault plane azimuth from experimental data for eleven explosions. Experimental data smoothed. S=1.25.

Fig. 5. Cup.

Fig. 6. Bronze.

Fig. 6a. Bronze, finer contour.

Fig. 7. Corduroy.

Fig. 8. Buff.

Fig. 9. Duryea.

Fig. 10. Chartreuse.

Fig. 11. Tan.

Fig. 11a. Tan, finer contour.

Fig. 12. Half Beak.

Fig. 12a. Half Beak, finer contour.

Fig. 13. Greeley.

Fig. 14. Faultless.

Fig. 15. Boxcar.

Fig. 16. L/R radiation pattern produced by either a right-lateral strike-slip fault at 166 degrees or a left-lateral strike-slip fault at 76 degrees.

Figs. 17 - 27. L/R radiation patterns for vertical strike-slip faults for eleven explosions. Scale factor, S=1.25. Fault orientation Ψ is that of the best fitting right-lateral fault for each explosion. F is the part double-couple. Crosses are experimental (unsmoothed) points. Numbers at edge are data points which fall outside the plots. Note: The radial scales on the polar plots are not all the same.

	Event	F	Ψ
Fig. 17.	Cup	.6	112
Fig. 18.	Bronze	.36	13
Fig. 19.	Corduroy	.6	166
Fig. 20.	Buff	.38	28
Fig. 21.	Duryea	.56	168
Fig. 22.	Chartreuse	.63	179
Fig. 23.	Tan	.36	154
Fig. 24.	Half Beak	.57	160
Fig. 25.	Greeley	.9	180
Fig. 26.	Faultless	.36	102
Fig. 27.	Boxcar	.45	160

Figs. 28 - 31. Contour plots of part double-couple versus fault azimuth for the explosion Corduroy for various values of the scale factor S.

Fig. 28. S = .5

Fig. 29. S = 1.0

Fig. 30. S = 1.5

Fig. 31. S = 2.0

Fig. 32. Generalized geologic map of the Nevada Test Site with the location of explosions in relation to major faults.

Fig. 33. Yucca Flat with the fault plane solutions of three explosions in relation to the natural and explosion produced fracture trends.

Fig. 1. Rayleigh waves from the Greeley explosion on long-period vertical component at Resolute Bay, Canada.

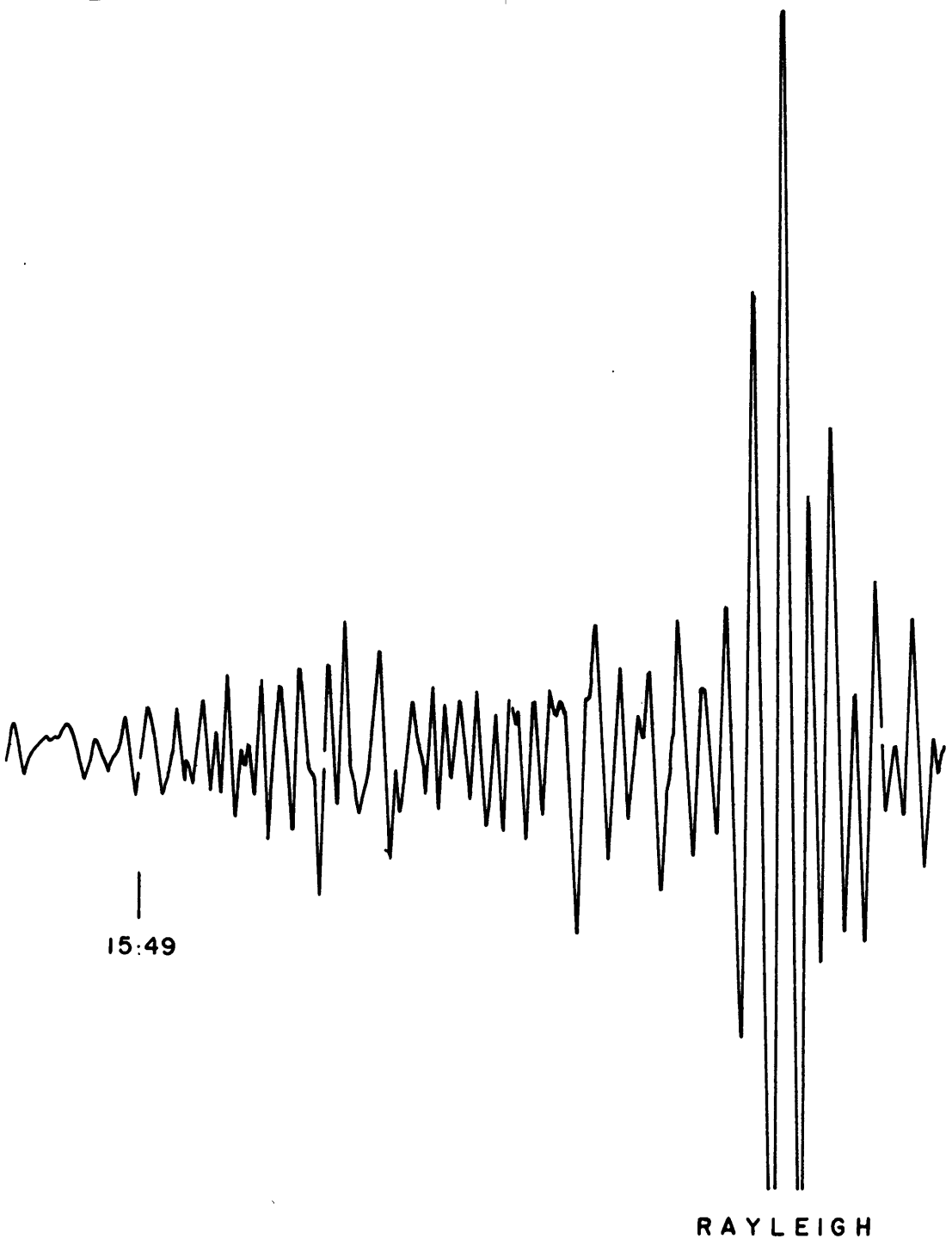
LPZ
15:49
RAYLEIGH

Fig. 2. Love and Rayleigh waves from the Greeley explosion on long-period north-south component at Resolute Bay, Canada.

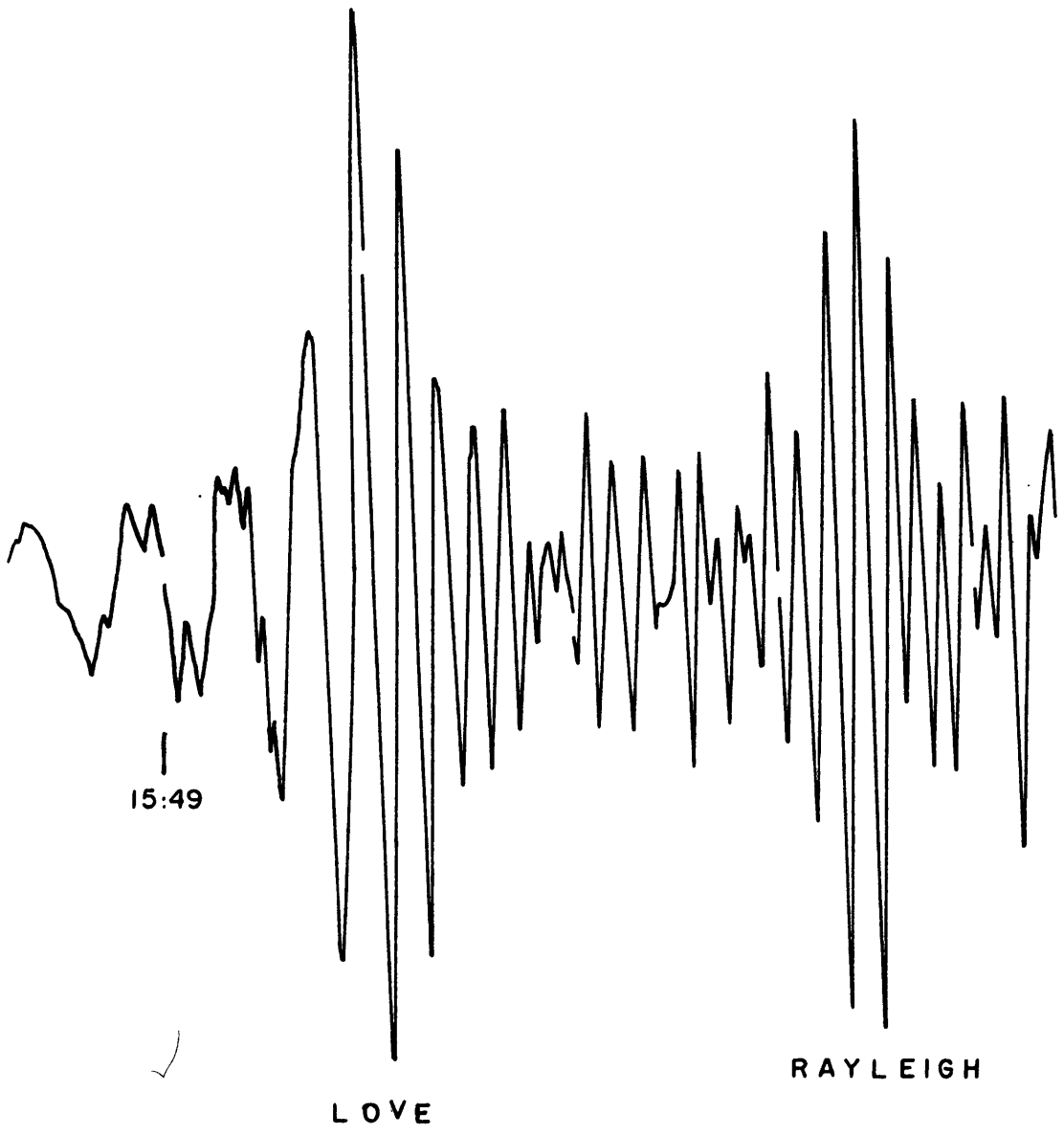
LPN
15:49
LOVE
RAYLEIGH

Fig. 3. Love waves from the Greeley explosion on long-period east-west component at Resolute Bay, Canada.

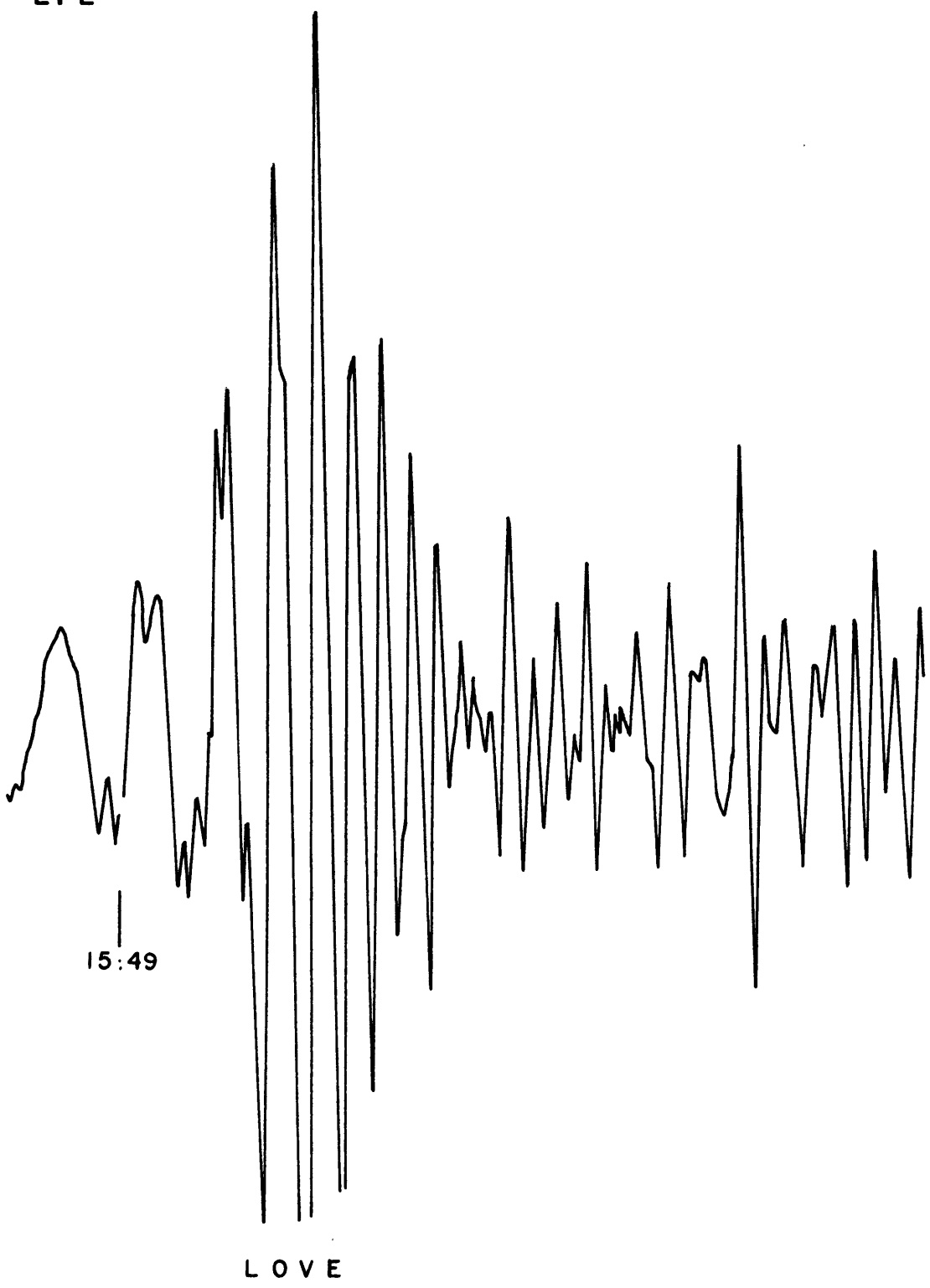
LPE
15:49
LOVE

Fig. 4. Contour plot of deviations of combinations of part double-couple and fault plane azimuth from experimental data for the explosion Corduroy. Experimental data not smoothed. Scale factor, S=1.25.

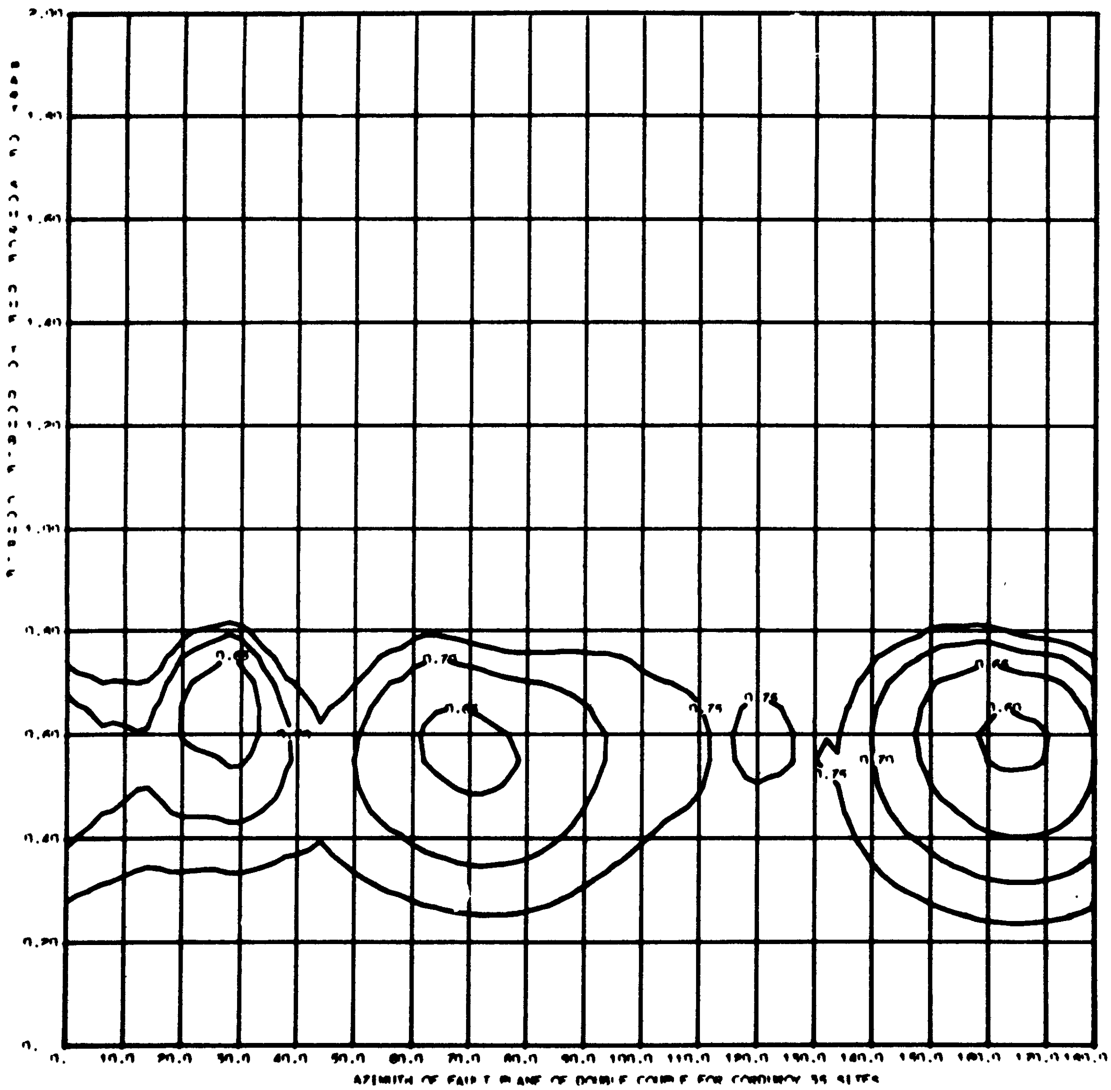

Figs. 5 - 15. Contour plots of deviations of combinations of part double-couple and fault plane azimuth from experimental data for eleven explosions. Experimental data smoothed. Scale factor, S=1.25.

Fig. 5. Cup.

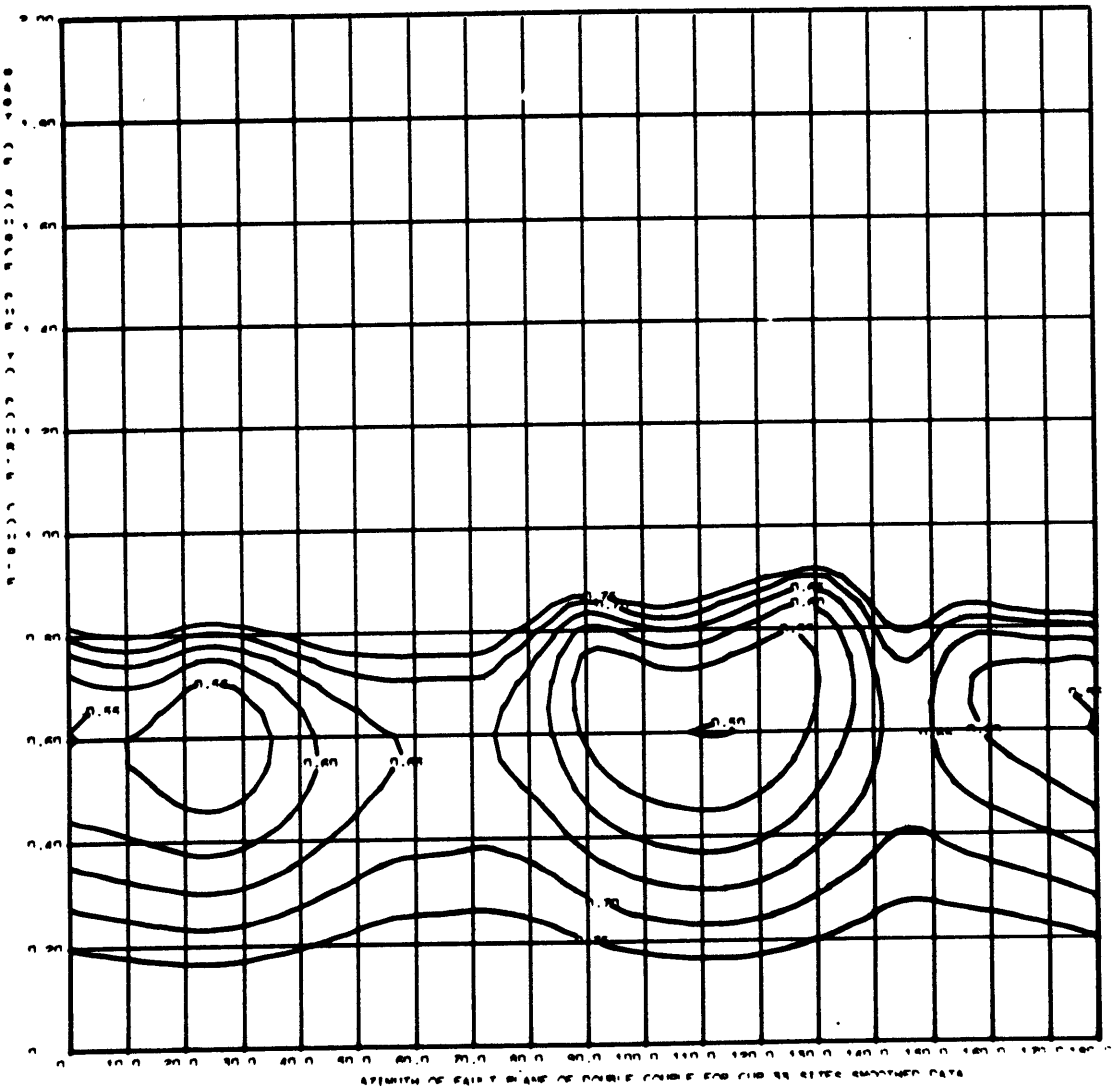

Fig. 6. Bronze.

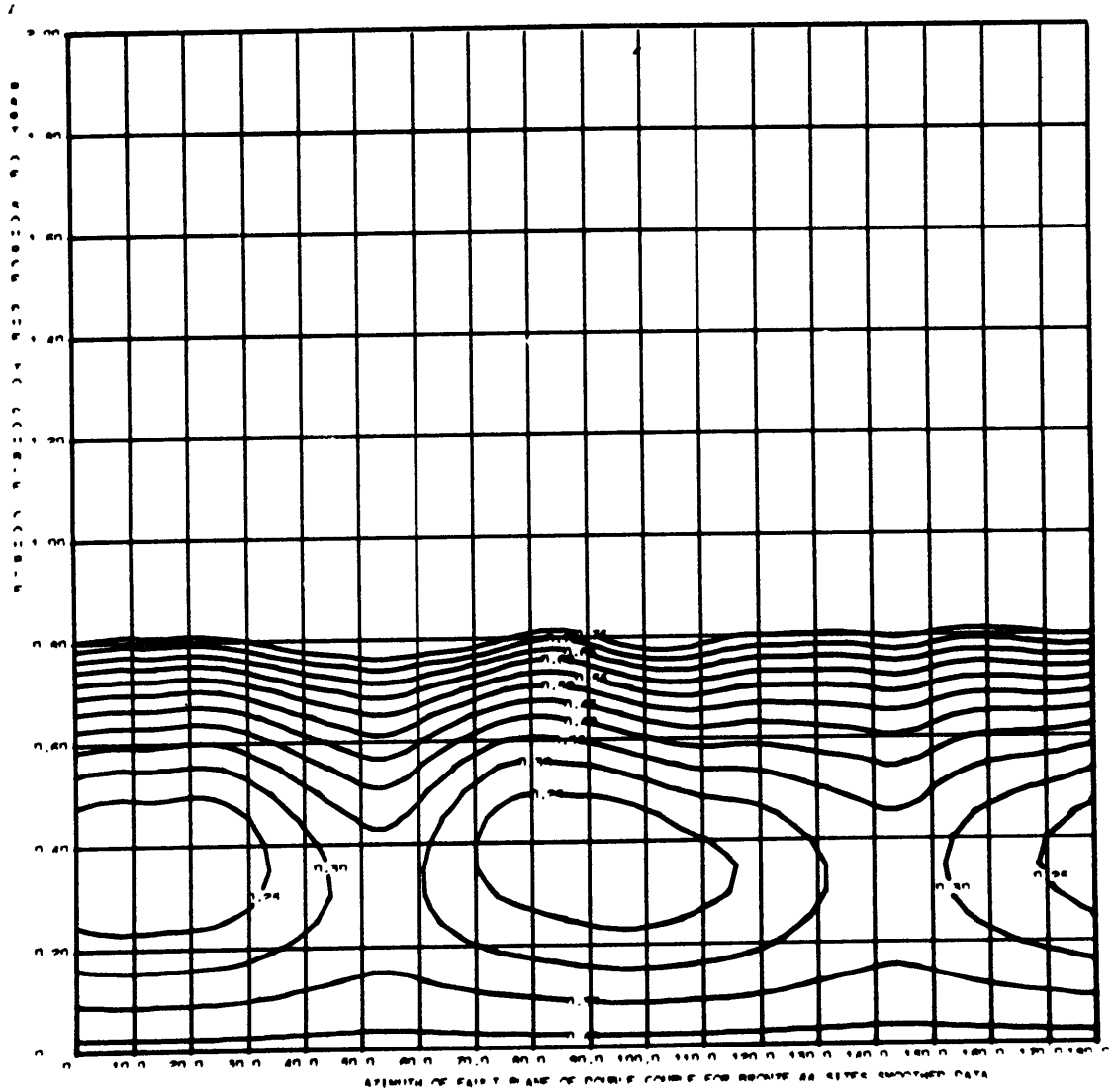

Fig. 6a. Bronze, finer contour.

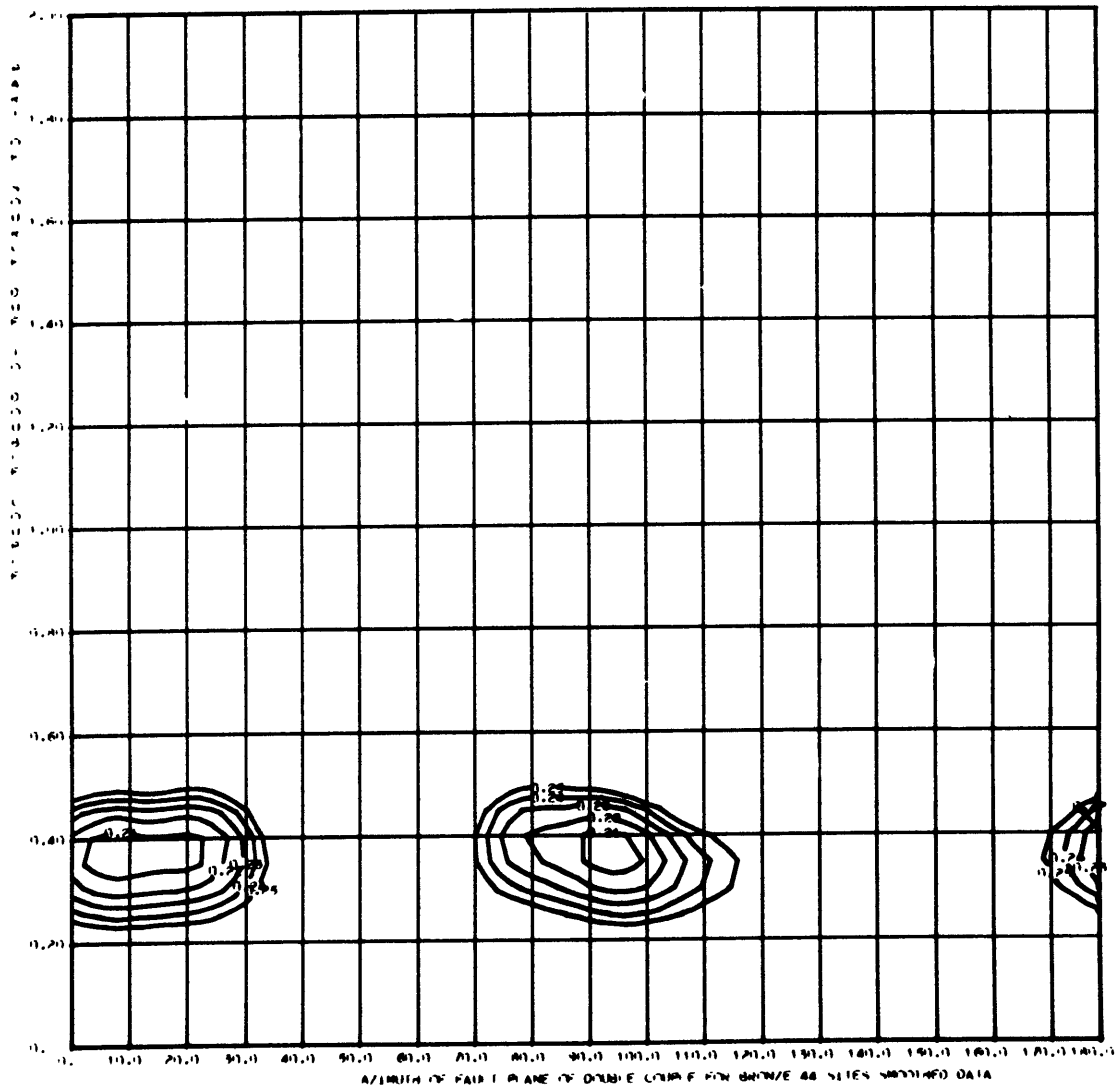

Fig. 7. Corduroy.

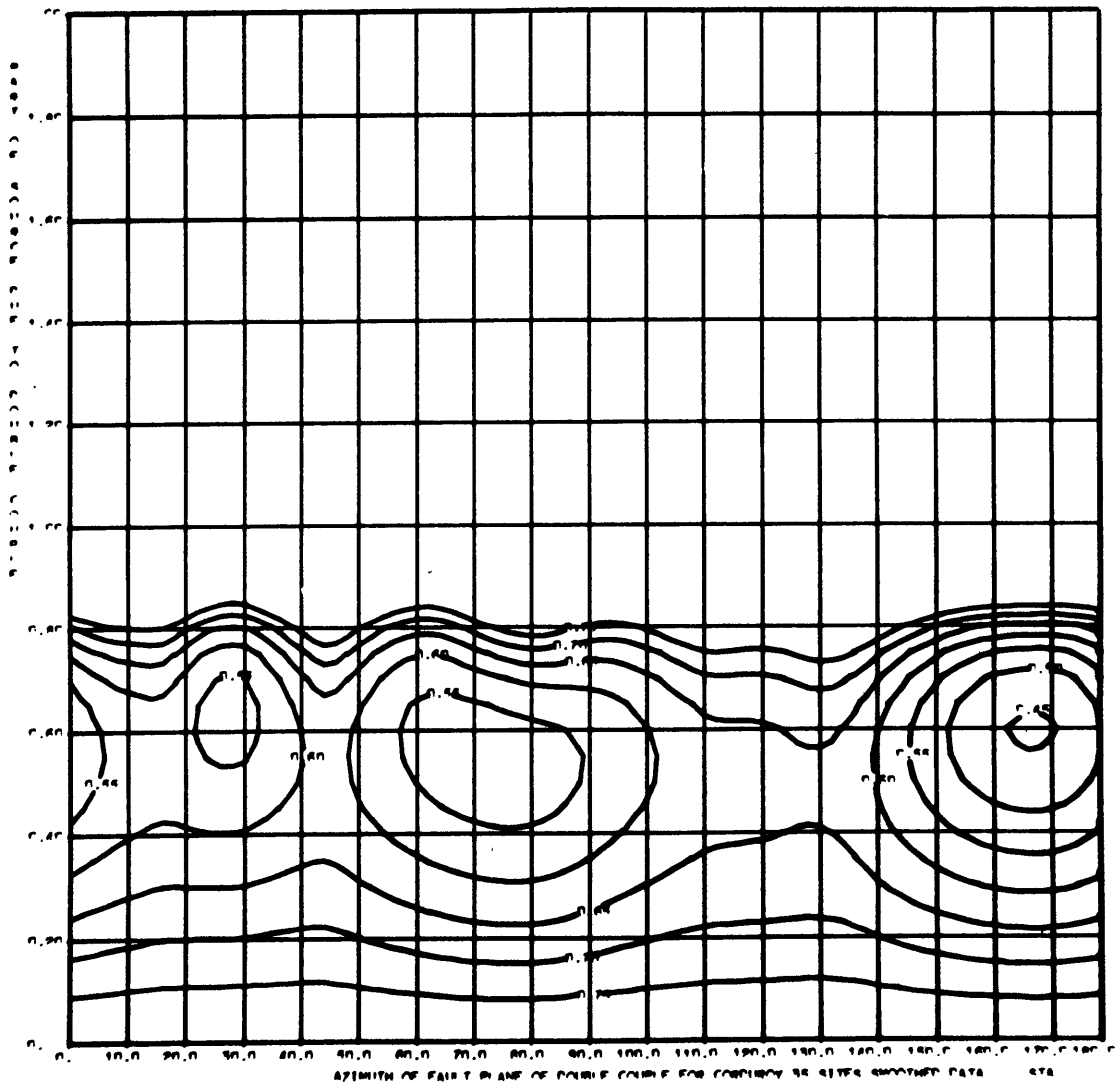

Fig. 8. Buff.

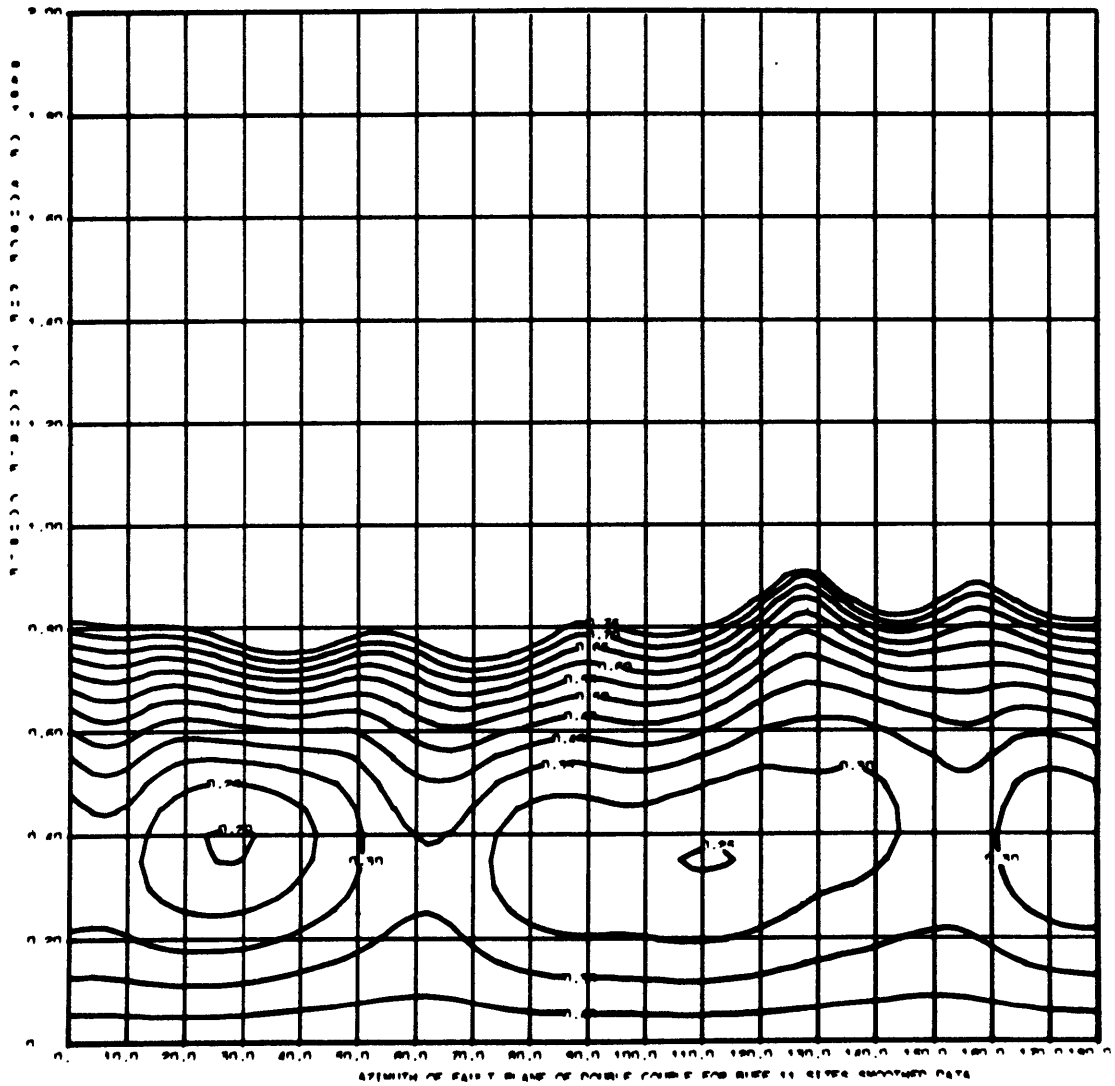

Fig. 9. Duryea.

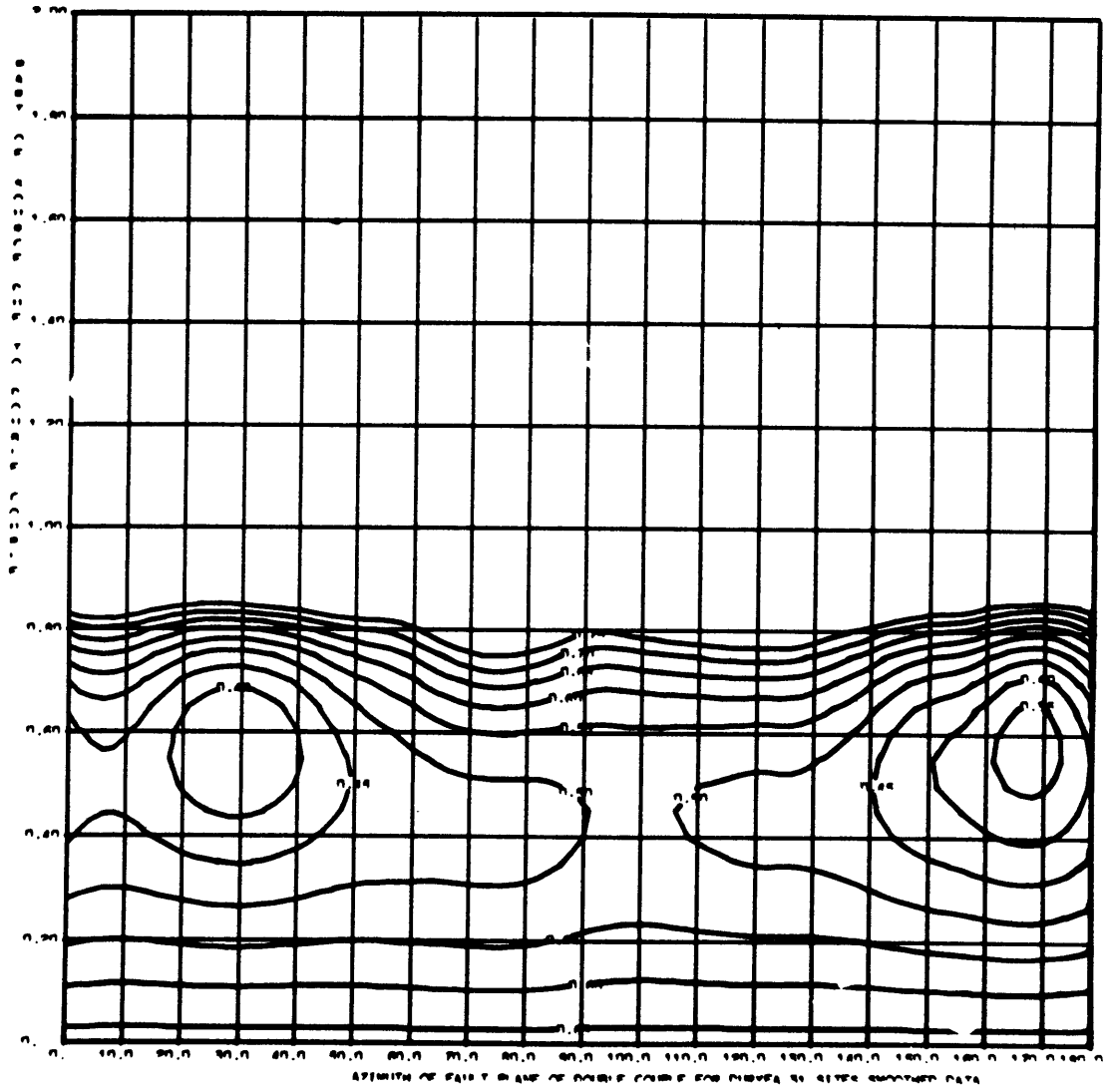

Fig 10. Chartreuse.

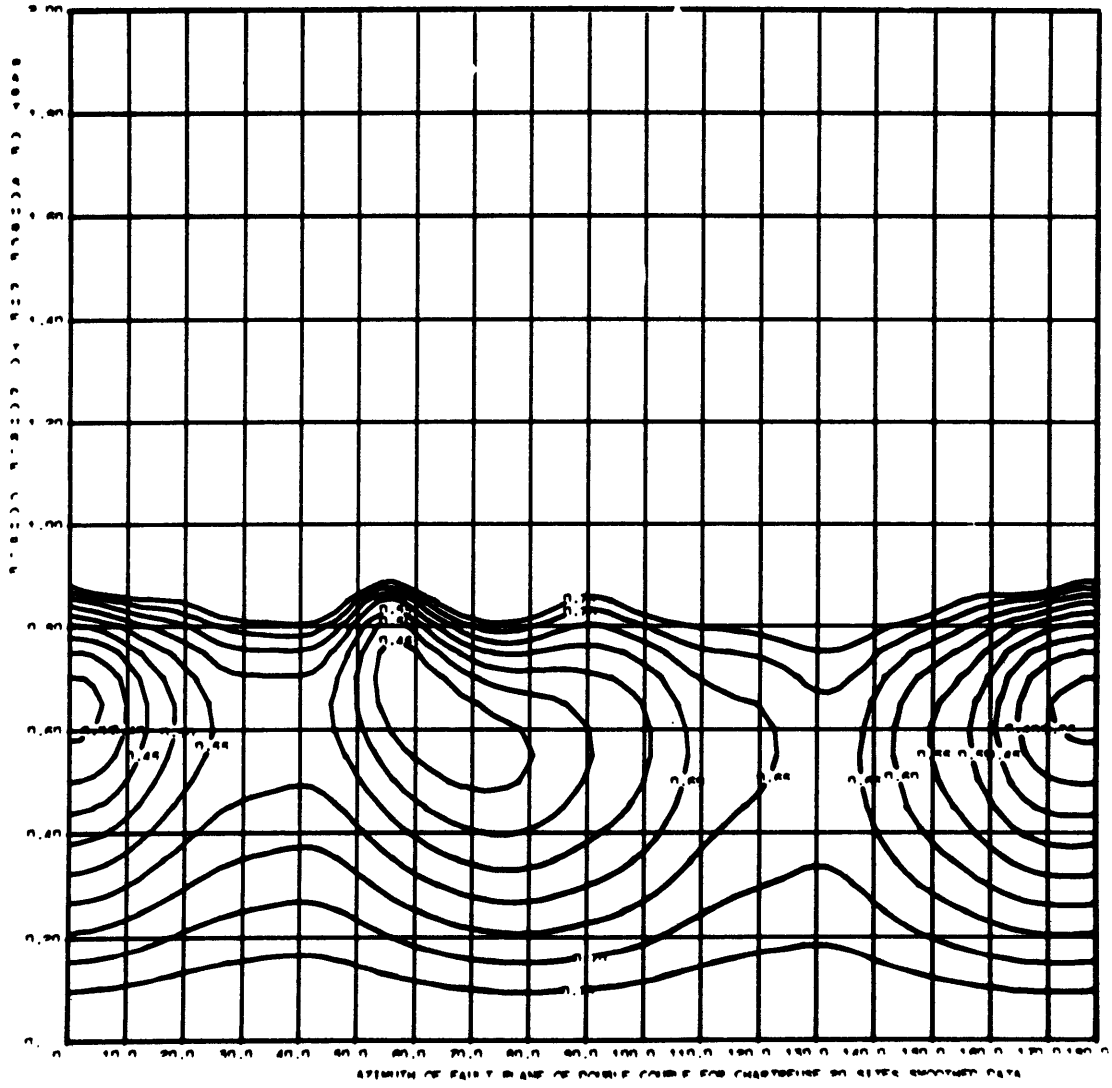

Fig. 11. Tan.

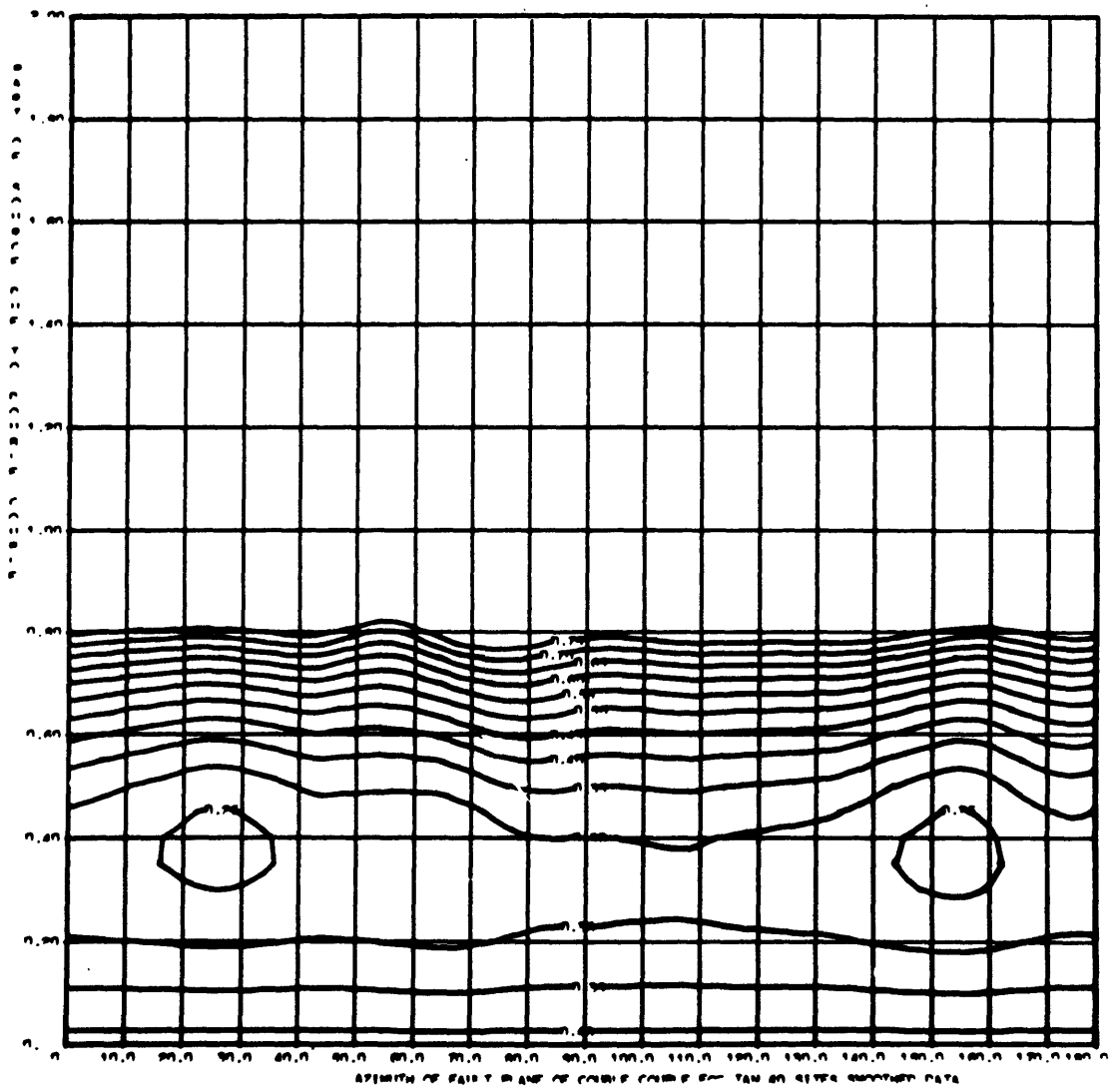

Fig. 11a. Tan, finer contour.

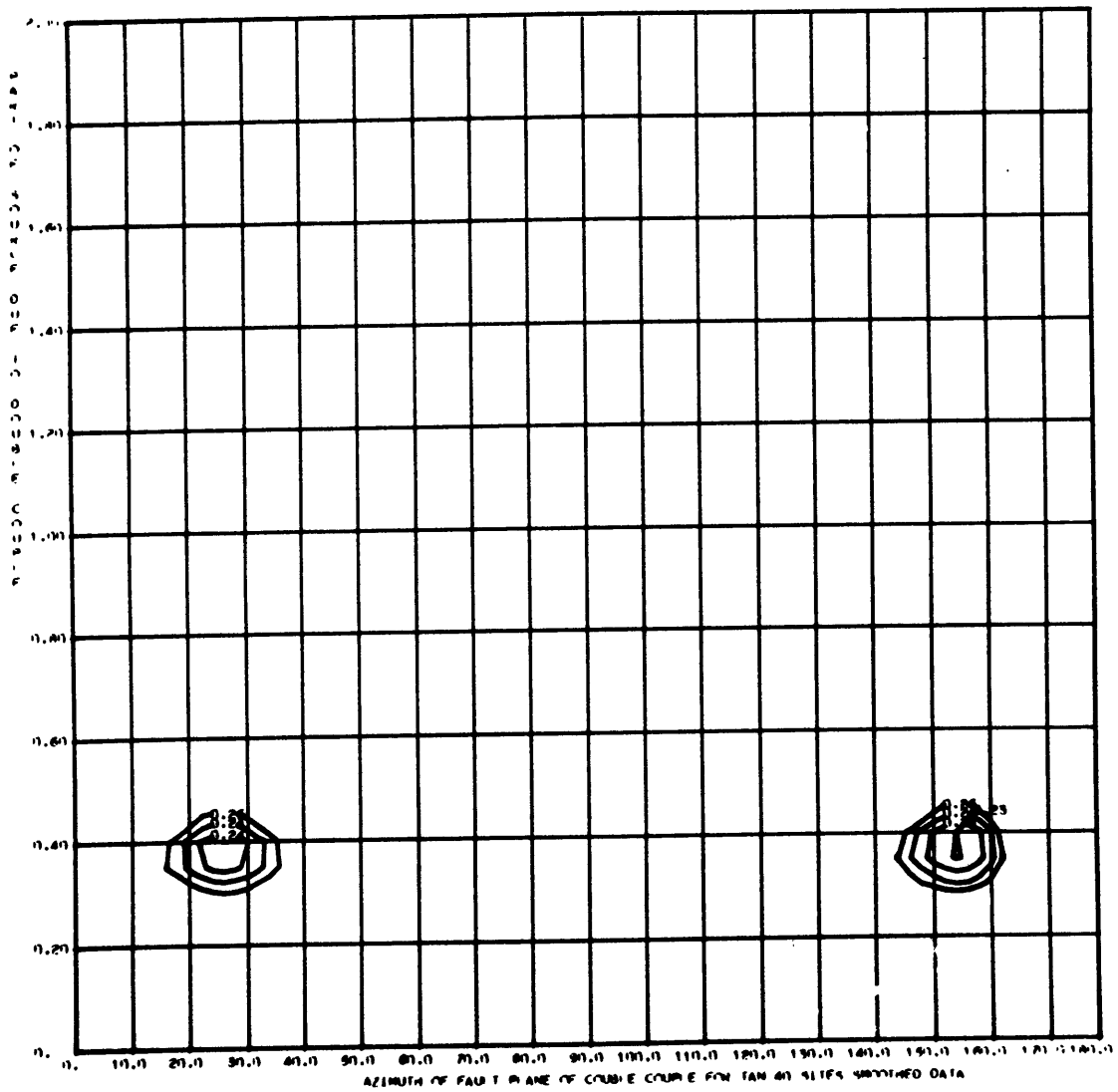
0.20
0.40
0.60
0.80
1.00
1.20
1.40
1.60
1.80
2.00
0.
10.0
20.0
30.0
40.0
50.0
60.0
70.0
80.0
90.0
100.0
110.0
120.0
130.0
140.0
150.0
160.0
170.0
180.0

Fig. 12. Half Beak.

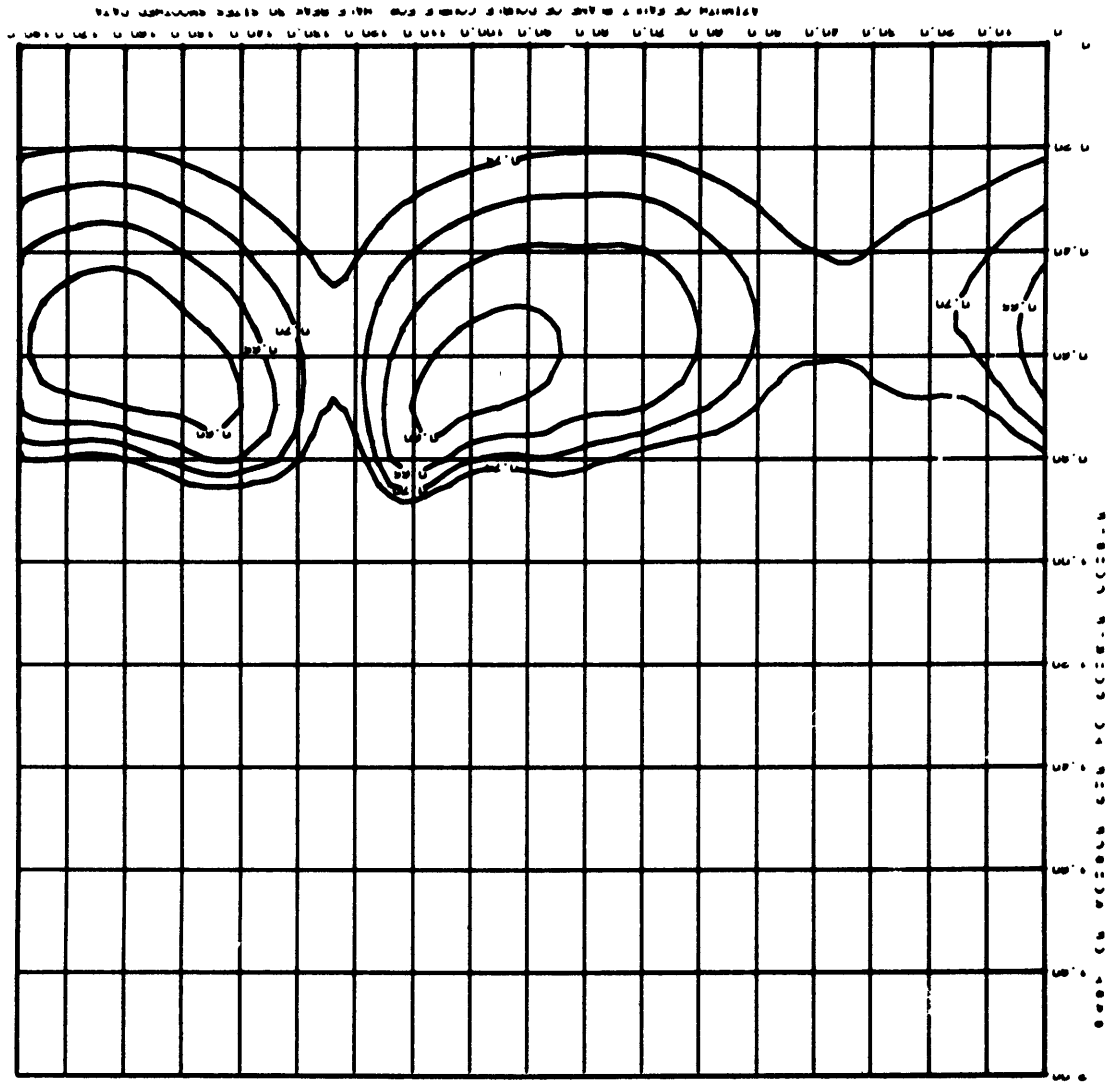

Fig. 12a. Half Beak, finer contour.

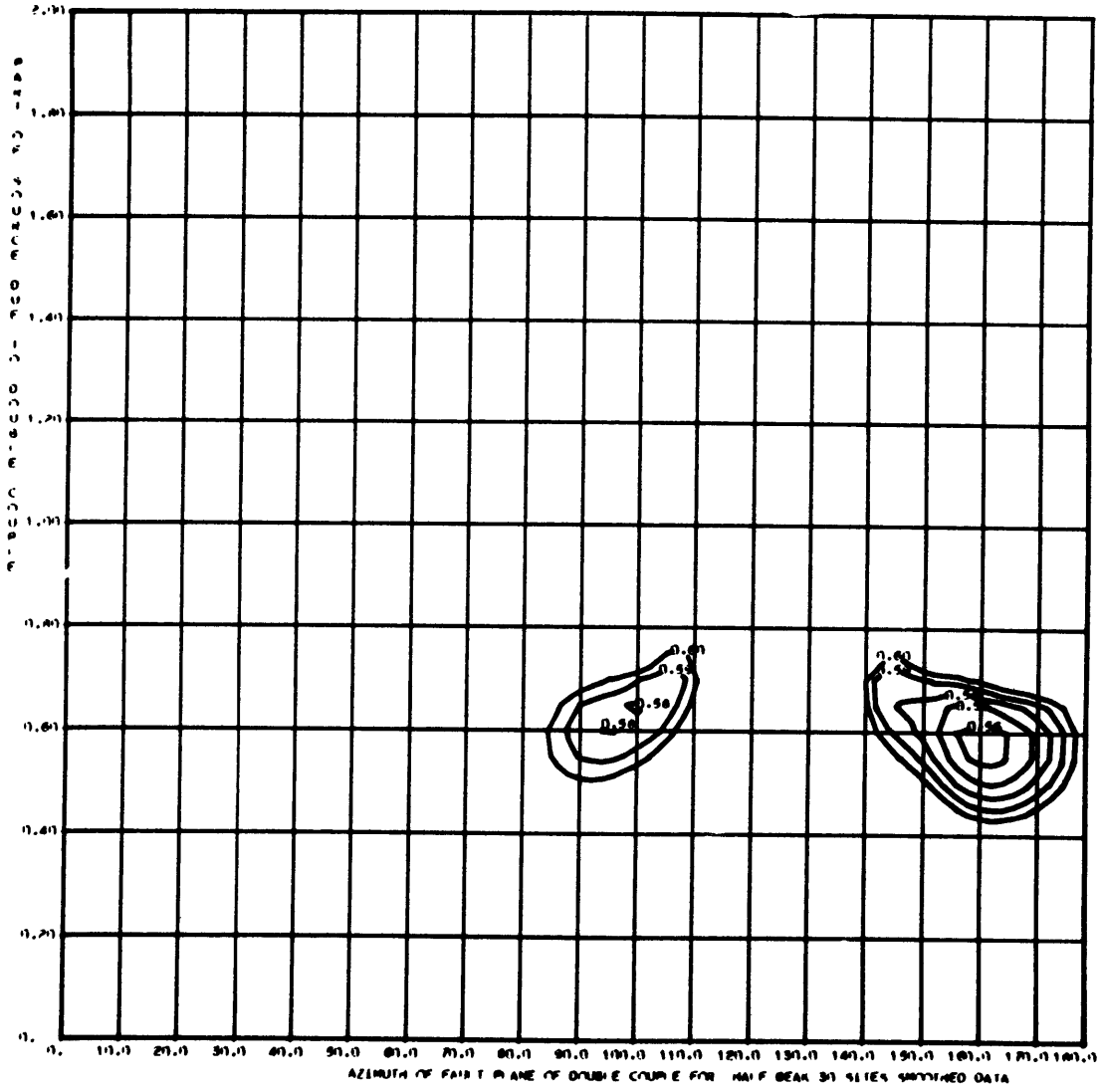
0.50
0.50
0.50
0.50
0.50
0.50
0.
10.0
20.0
30.0
40.0
50.0
60.0
70.0
80.0
90.0
100.0
110.0
120.0
130.0
140.0
150.0
160.0
170.0
180.0

Fig. 13. Greeley.

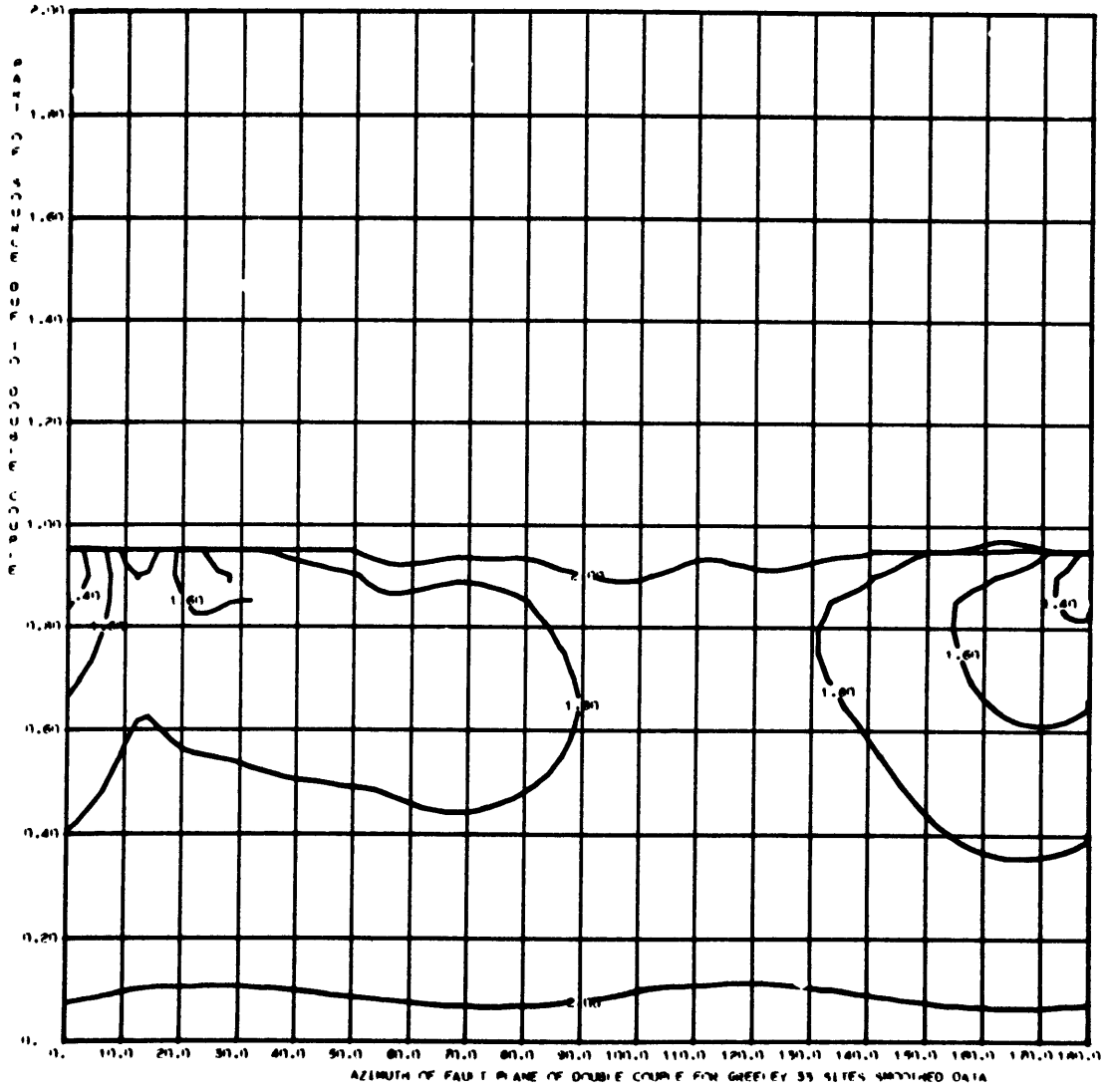
1.40
1.60
1.80
2.00
1.80
1.60
1.40
2.00
AZIMUTH OF FAULT PLANE OF DOUBLE COUPLE FOR GREELEY 33 SITES SMOOTHED DATA

Fig. 14. Faultless.

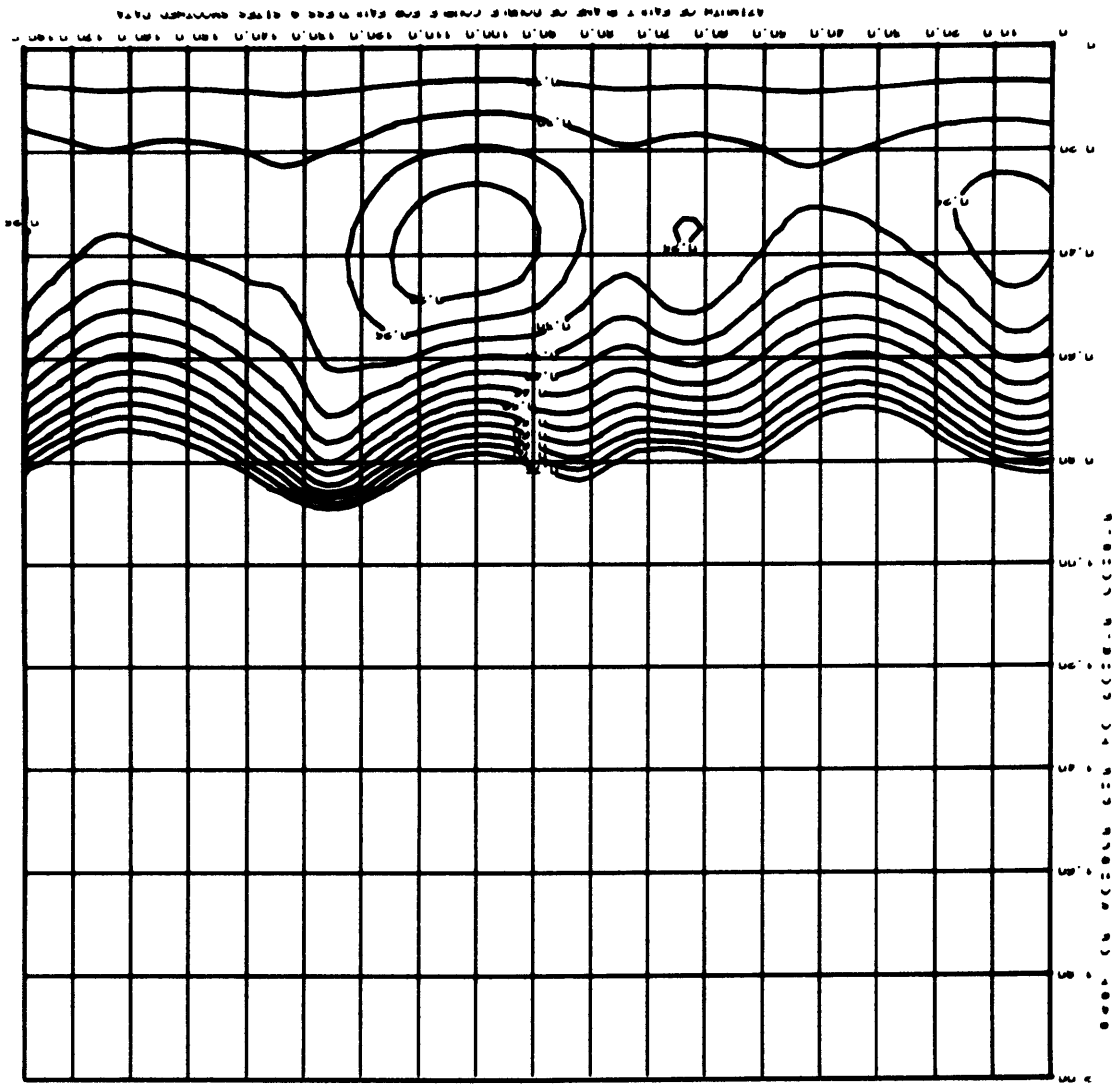

Fig. 15. Boxcar.

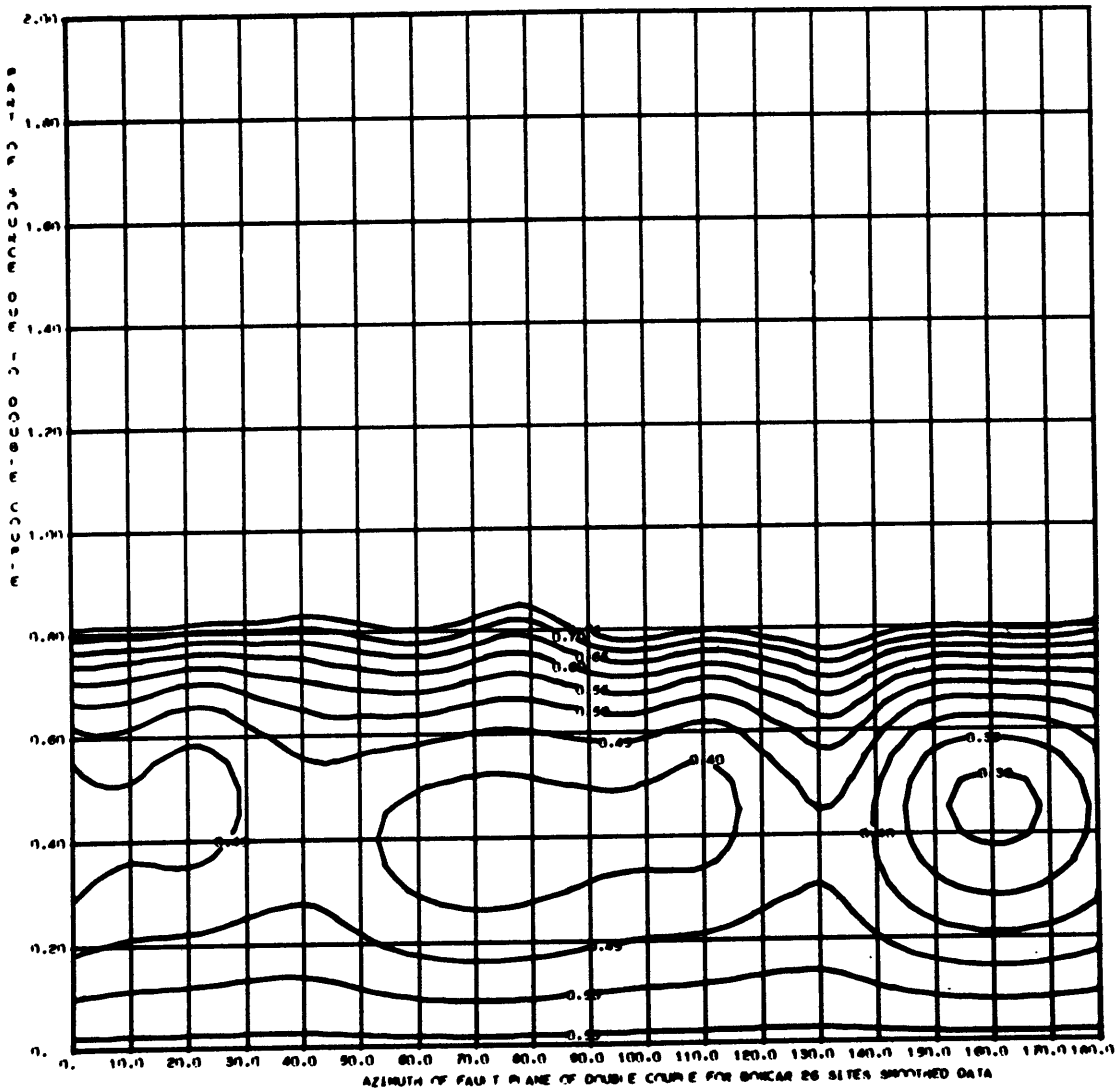
0.40
0.
10.0
20.0
30.0
40.0
50.0
60.0
70.0
80.0
90.0
100.0
110.0
120.0
130.0
140.0
150.0
160.0
170.0
180.0

Fig. 16. L/R radiation pattern produced by either a right-lateral strike-slip fault at 166 degrees or a left-lateral strike-slip fault at 76 degrees.

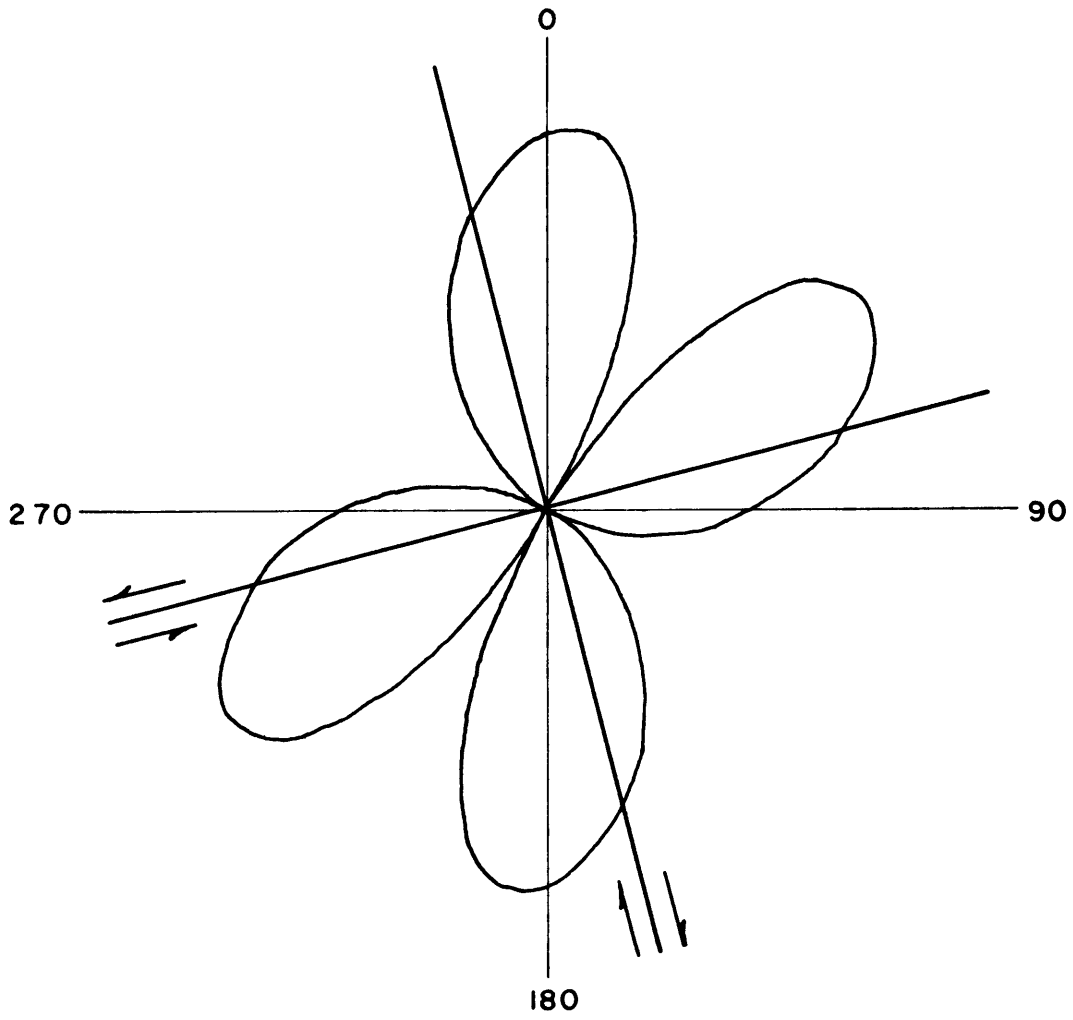
0
270
90
180

Figs. 17 - 27. L/R radiation patterns for vertical strike-slip faults for eleven explosions. Scale factor, S=1.25. Fault orientation ψ is that of the best fitting right-lateral fault for each explosion. F is the part double-couple. Crosses are experimental (unsmoothed) points. Numbers at edge are data points which fall outside the plots. Note: The radial scales on the polar plots are not all the same.

Event	F	ψ
Fig. 17. Cup	.6	112

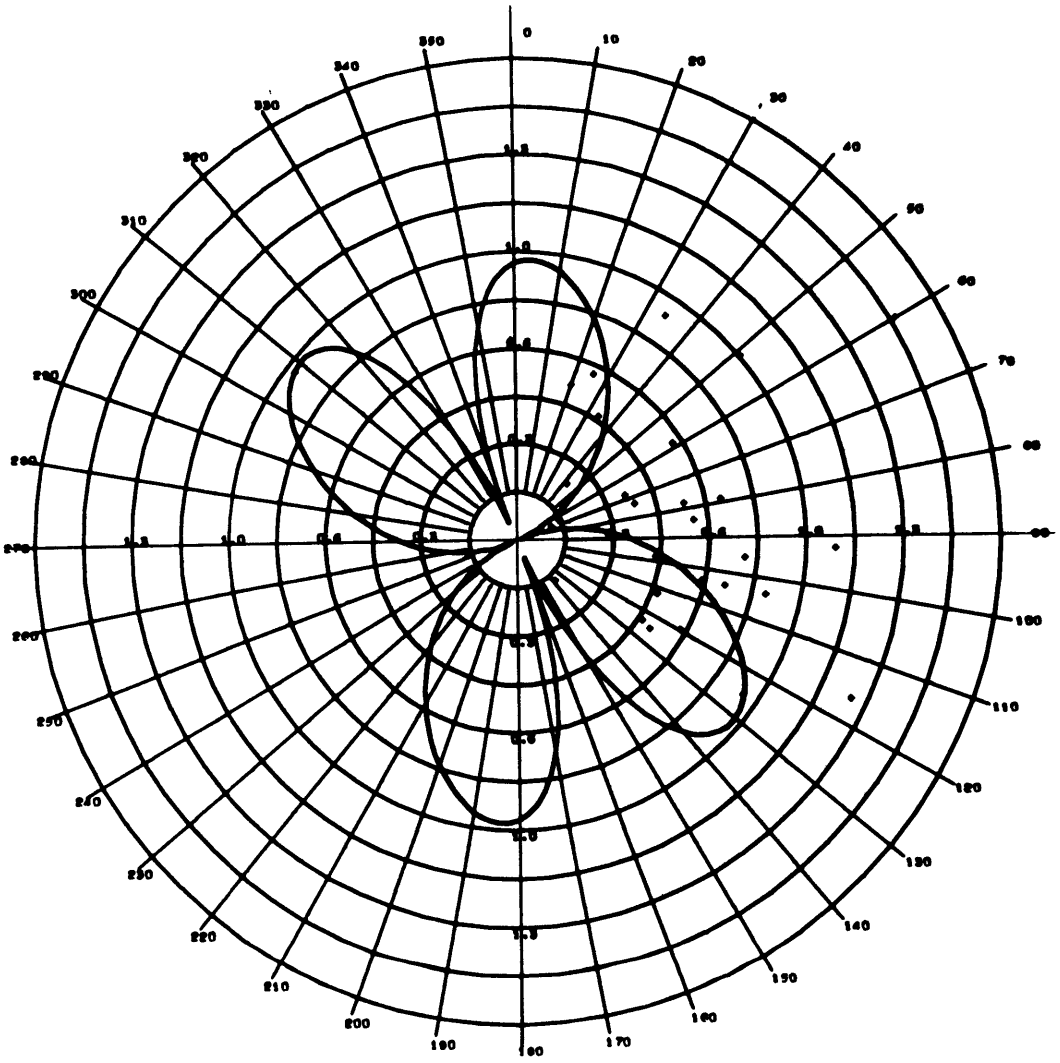
0
10
20
30
40
50
60
70
80
90
100
110
120
130
140
150
160
170
180
190
200
210
220
230
240
250
260
270
280
290
300
310
320
330
340
350

Fig. 18.	Bronze	.36	13

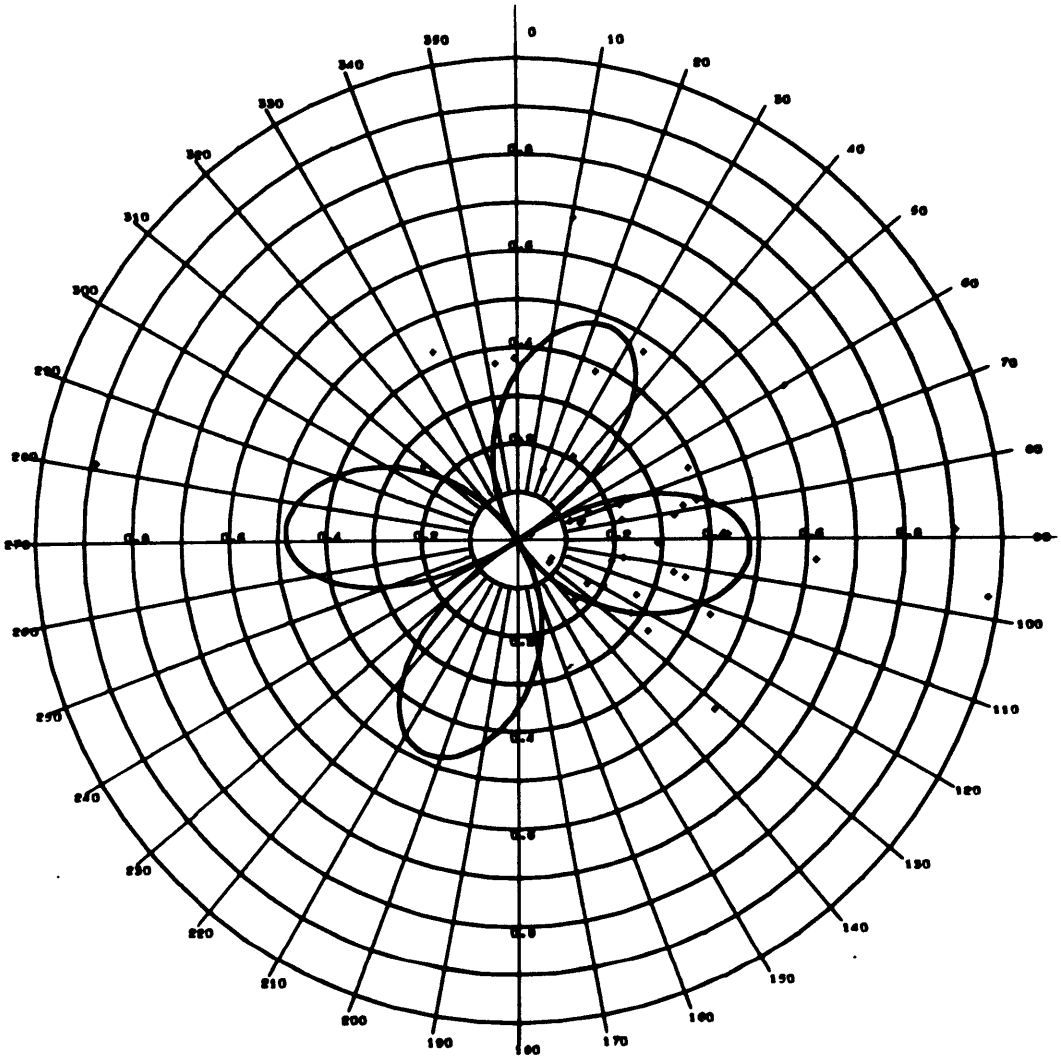
0
10
20
30
40
50
60
70
80
90
100
110
120
130
140
150
160
170
180
190
200
210
220
230
240
250
260
270
280
290
300
310
320
330
340
350

Fig. 19. Corduroy	.6	166

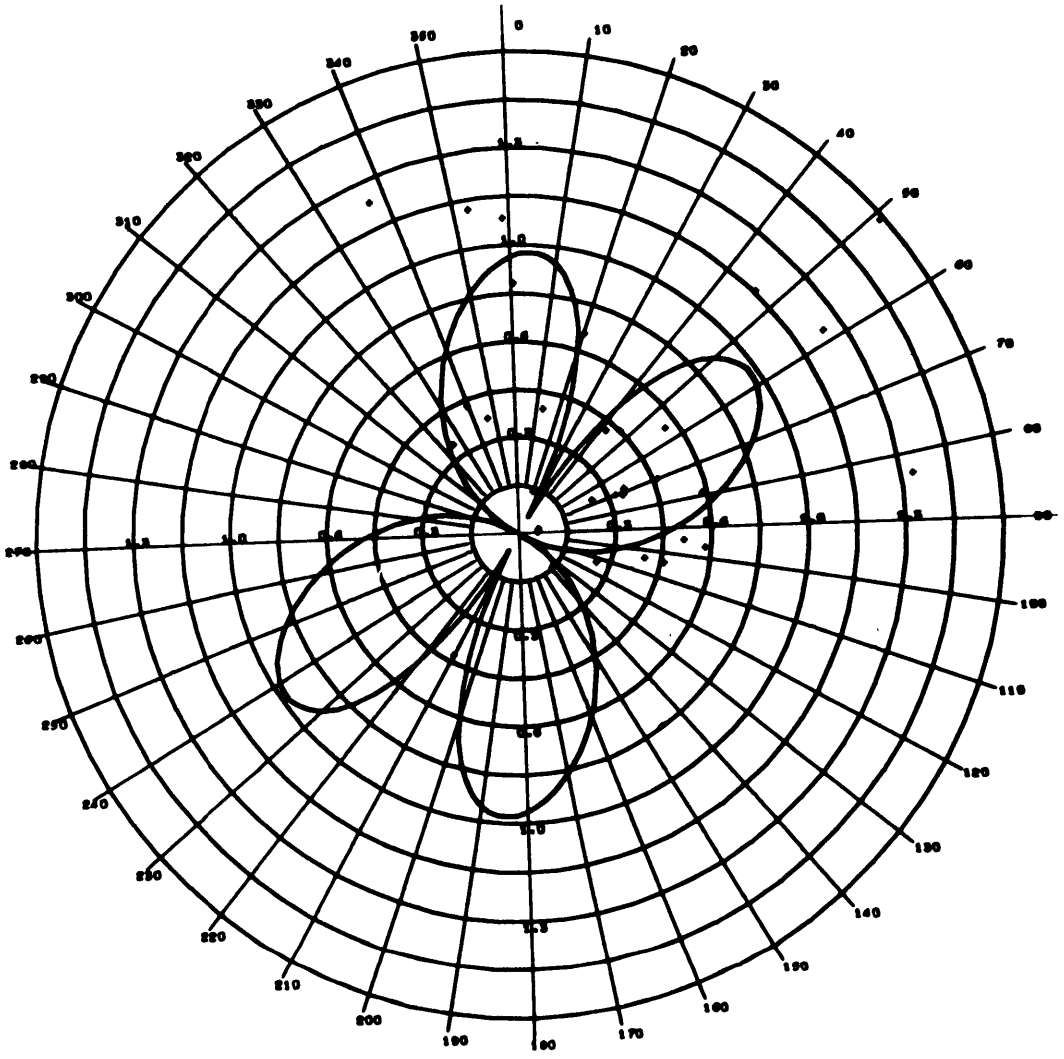
0
10
20
30
40
50
60
70
80
90
100
110
120
130
140
150
160
170
180
190
200
210
220
230
240
250
260
270
280
290
300
310
320
330
340
350

Fig. 20. Buff	.38	28

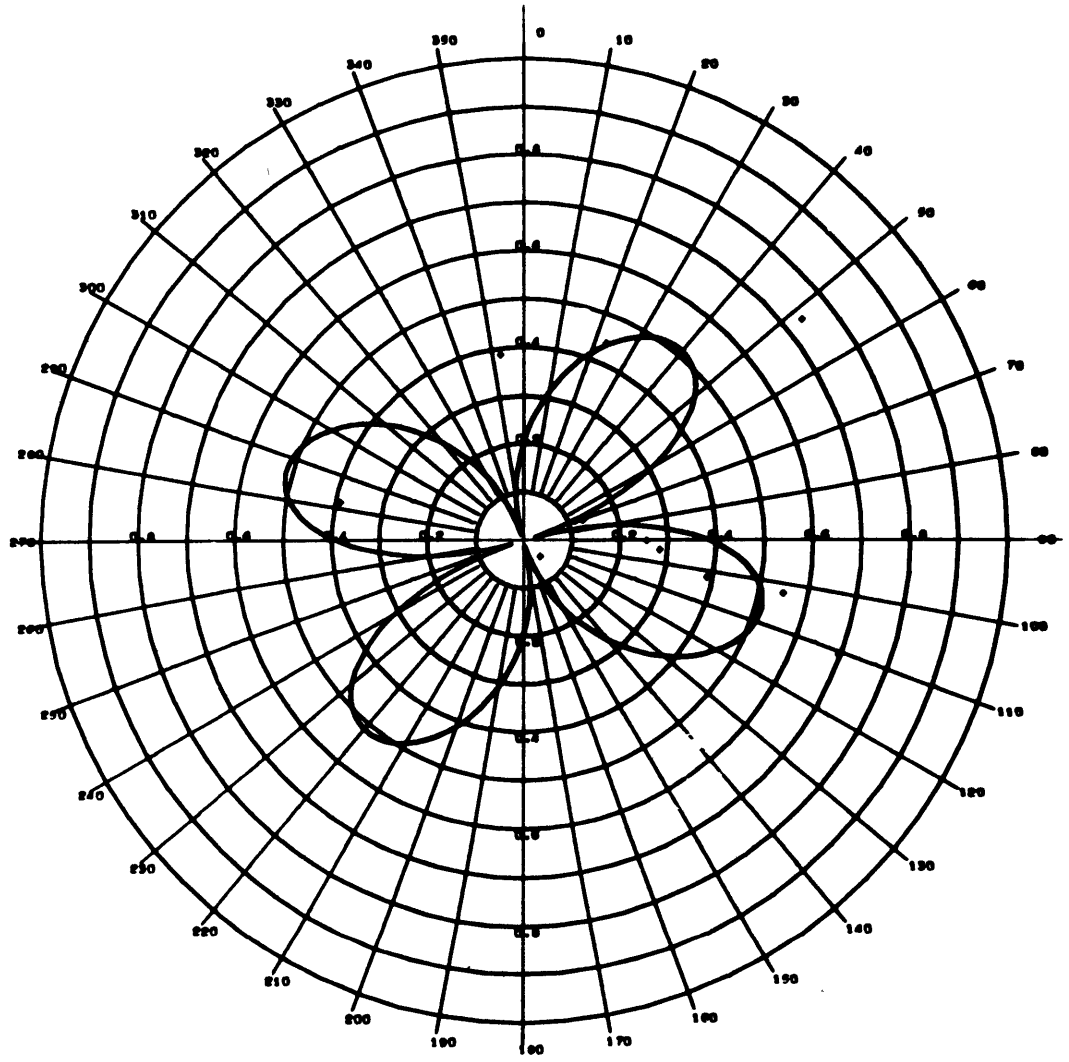
0
10
20
30
40
50
60
70
80
90
100
110
120
130
140
150
160
170
180
190
200
210
220
230
240
250
260
270
280
290
300
310
320
330
340
350

Fig. 21. Duryea	.56	168

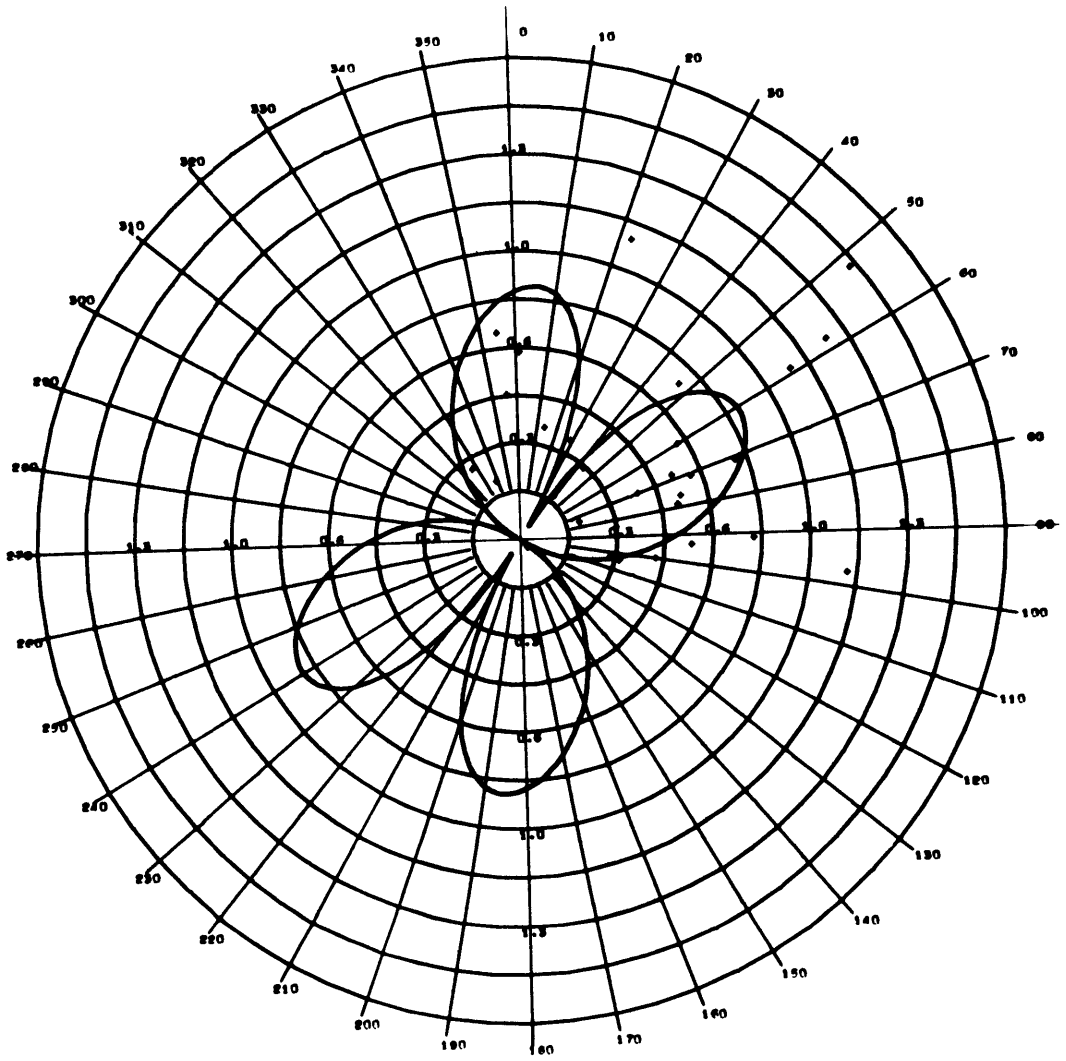
0
10
20
30
40
50
60
70
80
90
100
110
120
130
140
150
160
170
180
190
200
210
220
230
240
250
260
270
280
290
300
310
320
330
340
350

Fig. 22.	Chartreuse	.63	179

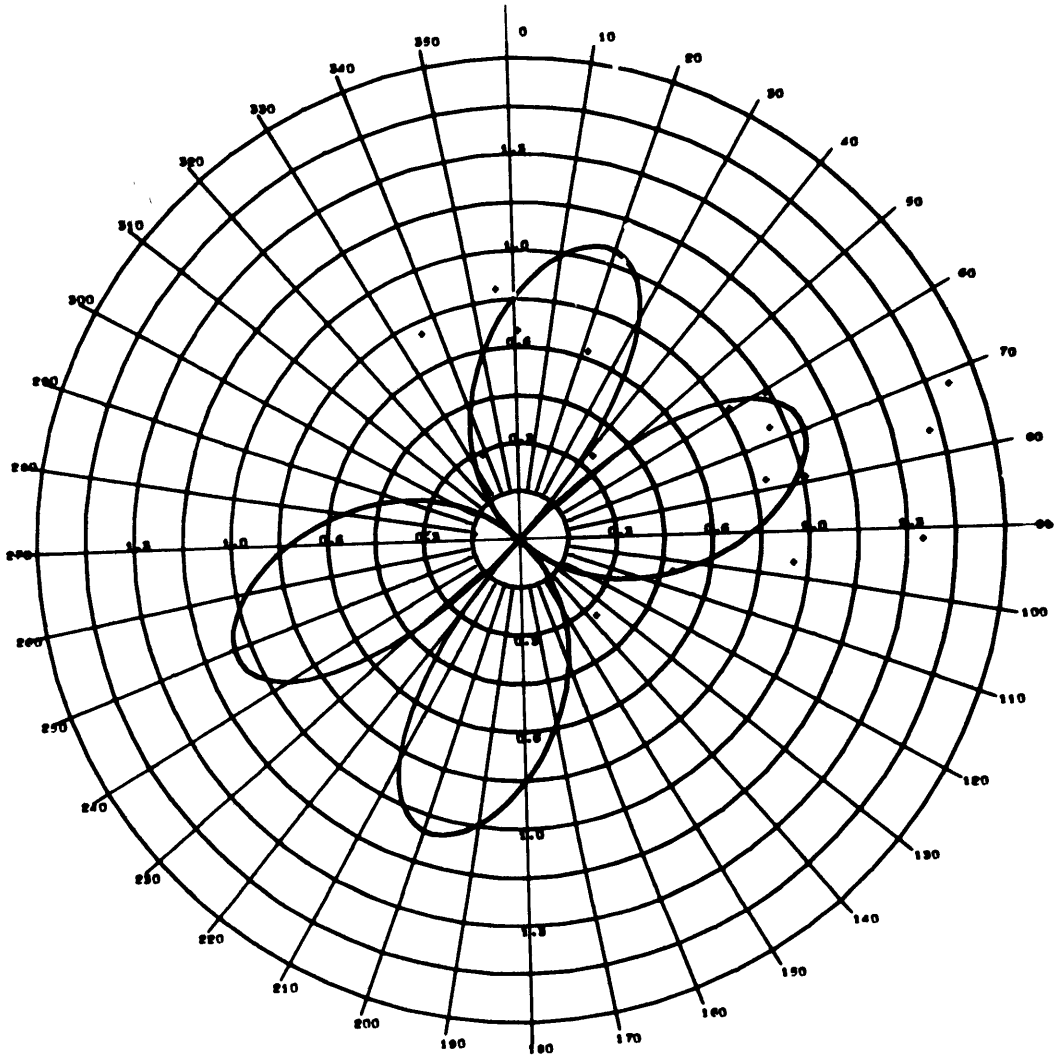
0
10
20
30
40
50
60
70
80
90
100
110
120
130
140
150
160
170
180
190
200
210
220
230
240
250
260
270
280
290
300
310
320
330
340
350

Fig. 23. Tan	.36	154

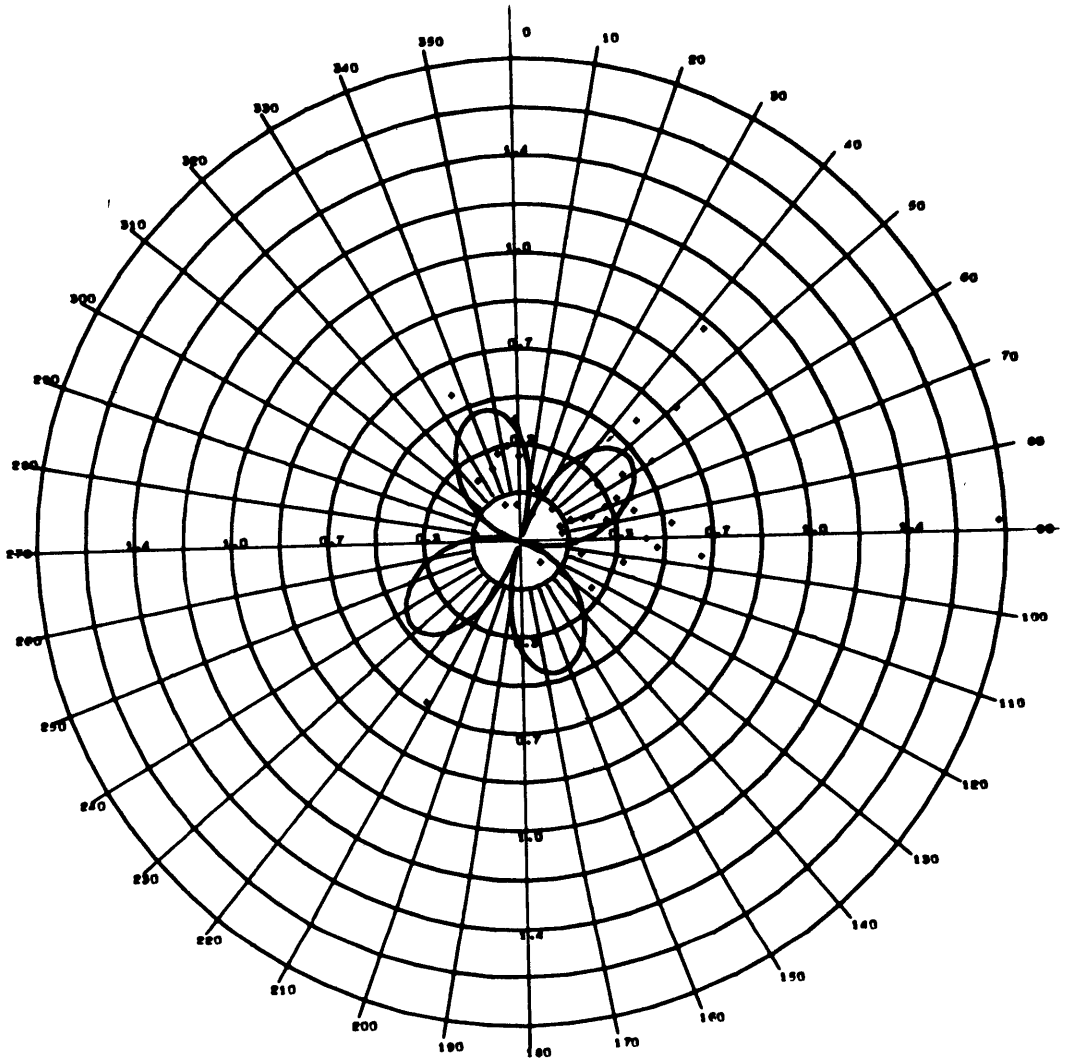
0
10
20
30
40
50
60
70
80
90
100
110
120
130
140
150
160
170
180
190
200
210
220
230
240
250
260
270
280
290
300
310
320
330
340
350

Fig. 24. Half Beak	.57	160

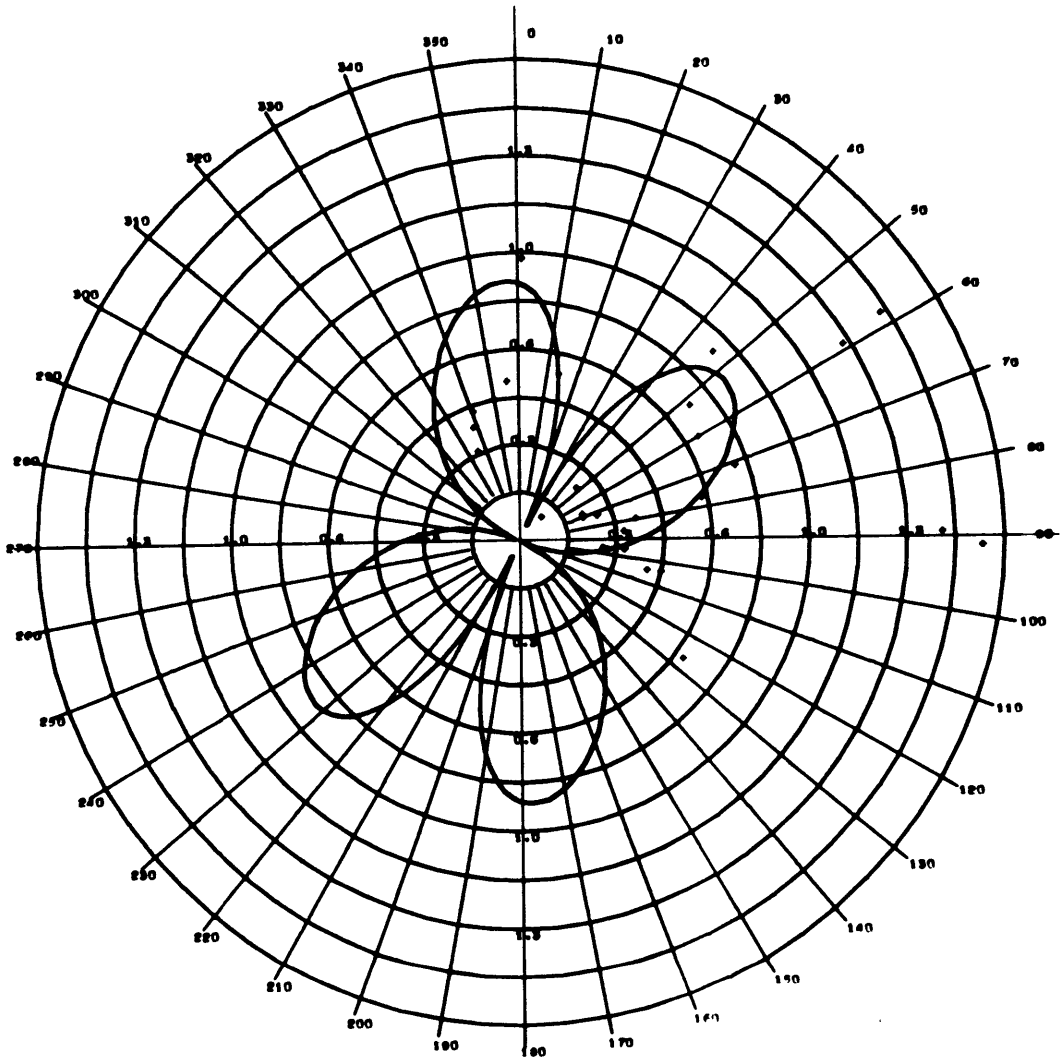
0
10
20
30
40
50
60
70
80
90
100
110
120
130
140
150
160
170
180
190
200
210
220
230
240
250
260
270
280
290
300
310
320
330
340
350

Fig. 25. Greeley .9 180

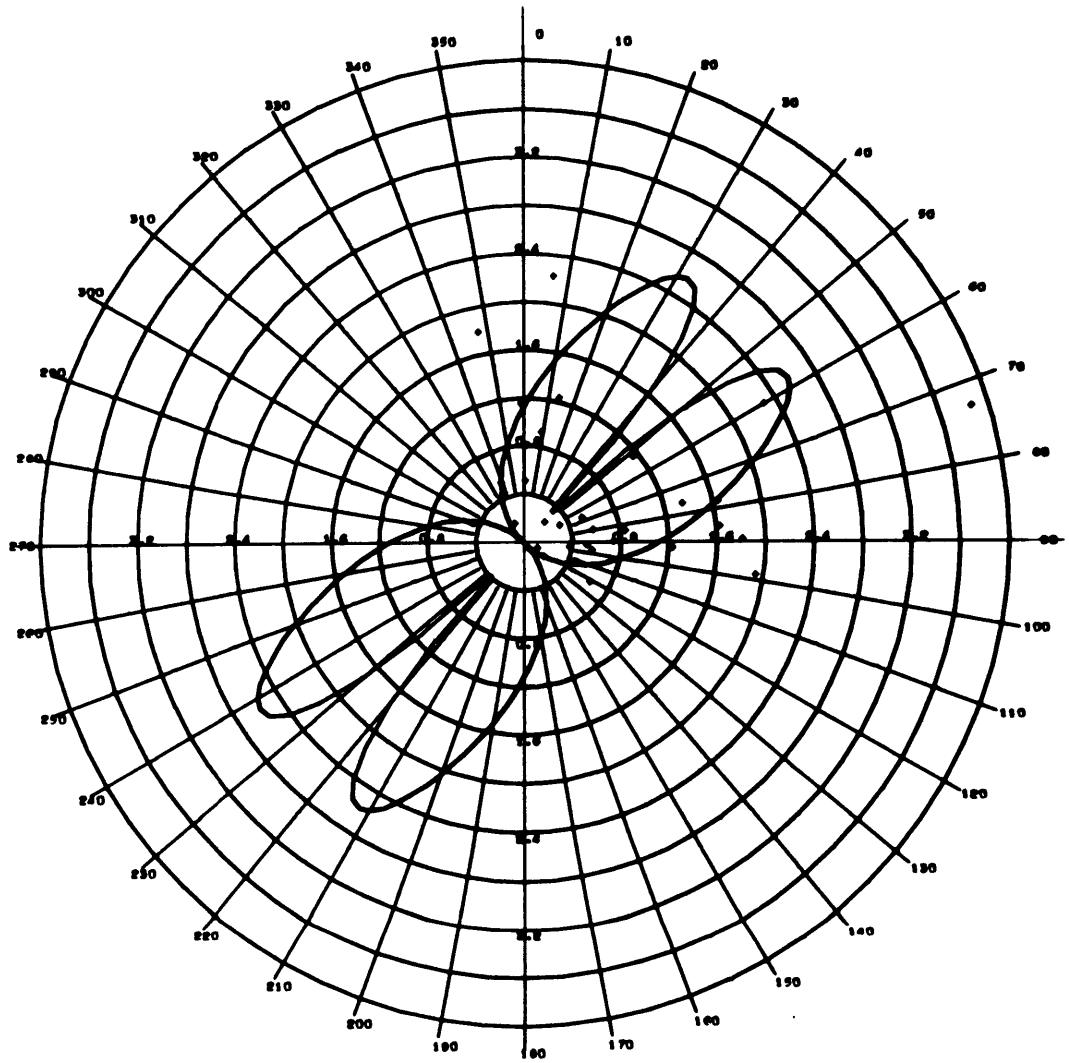

Fig. 26.	Faultless	.36	102

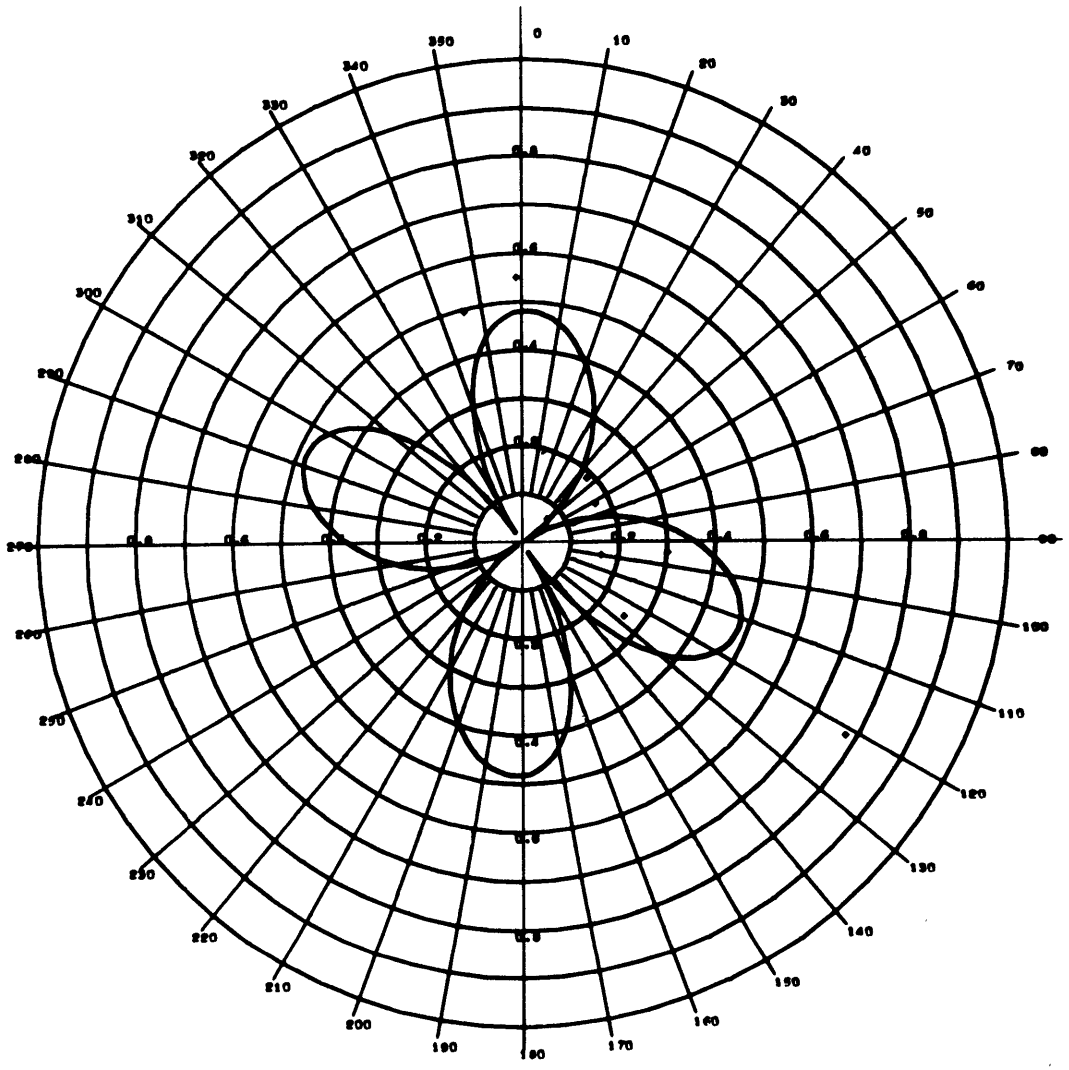
0
10
20
30
40
50
60
70
80
90
100
110
120
130
140
150
160
170
180
190
200
210
220
230
240
250
260
270
280
290
300
310
320
330
340
350

Fig. 27. Boxcar	.45	160

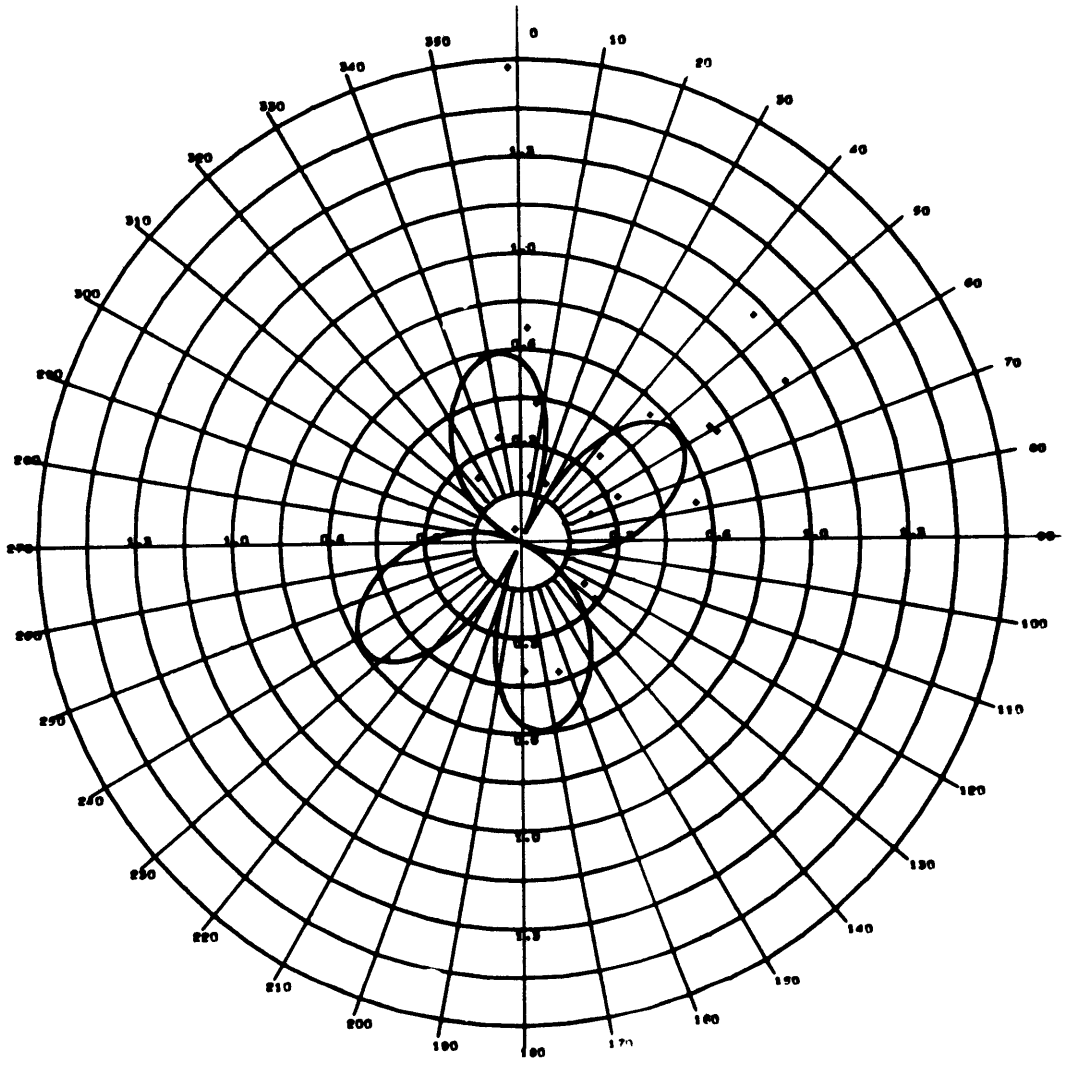
0
10
20
30
40
50
60
70
80
90
100
110
120
130
140
150
160
170
180
190
200
210
220
230
240
250
260
270
280
290
300
310
320
330
340
350

Figs. 28 - 31. Contour plots of part double-couple versus fault azimuth for the explosion Corduroy for various values of the scale factor S.

Fig. 28. S = .5

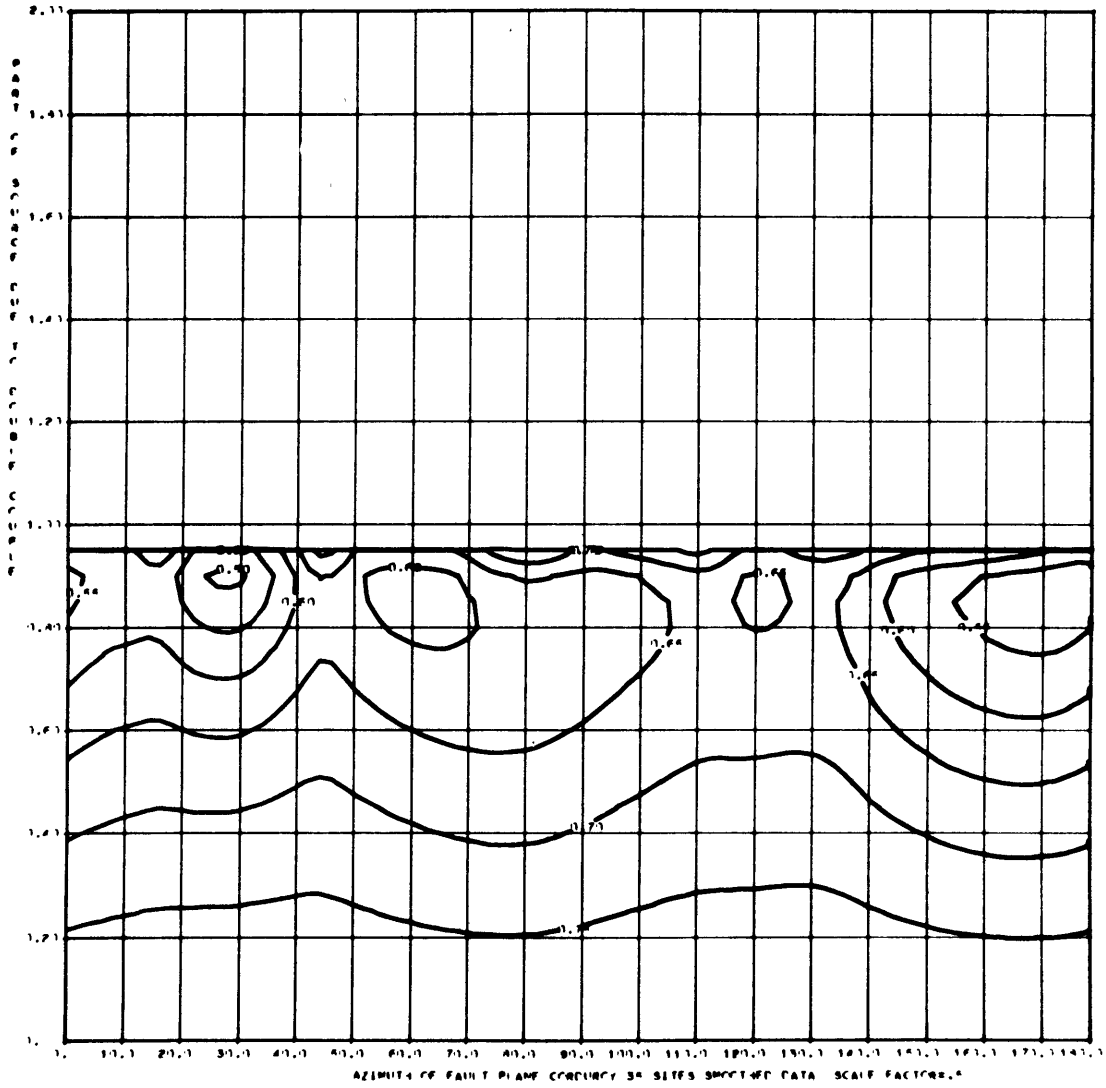
AZIMUTH OF FAULT PLANE CORDUROY 34 SITES SMOOTHED DATA SCALE FACTOR=.4

Fig. 29. S = 1.0

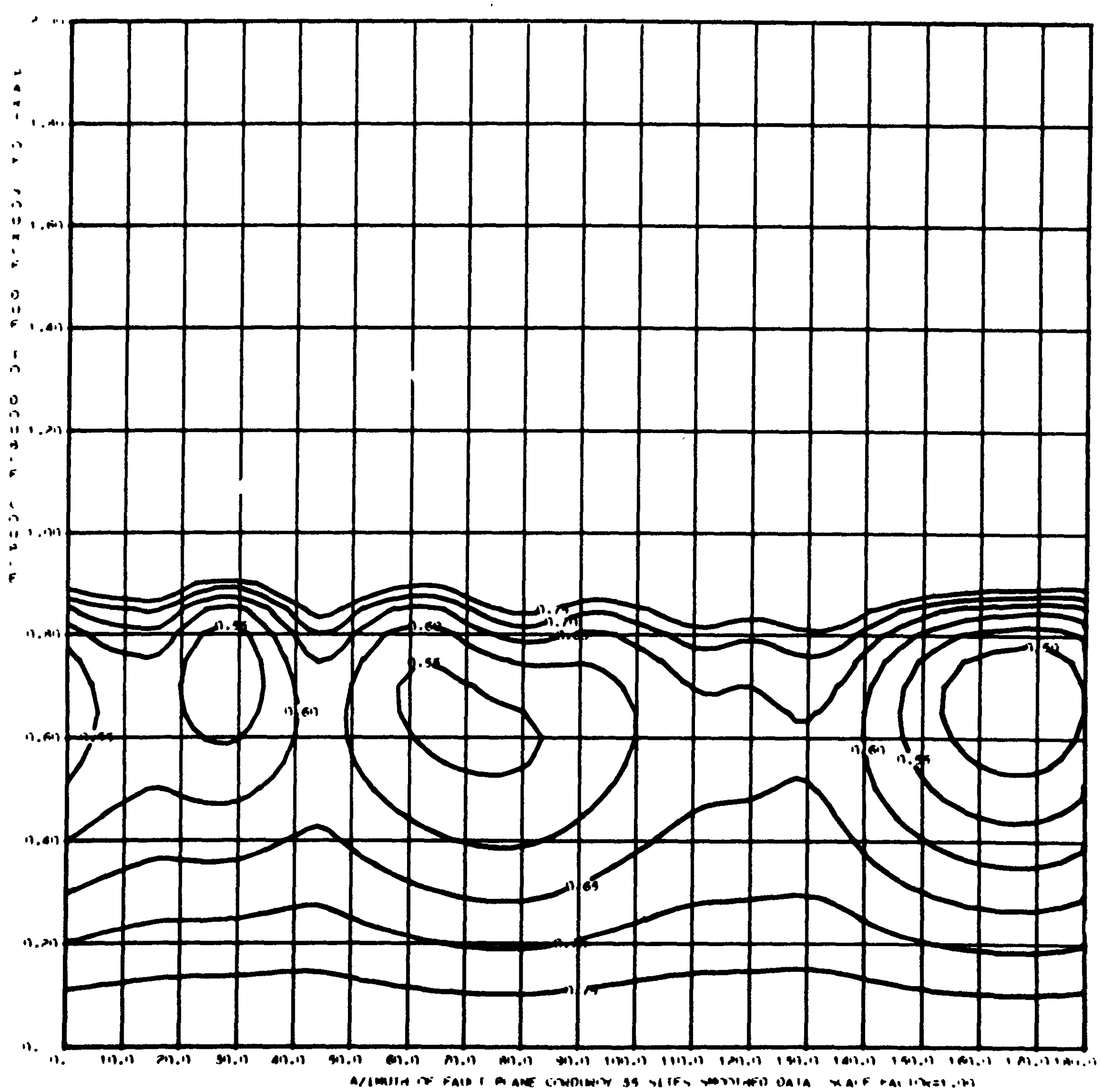

Fig. 30. S = 1.5

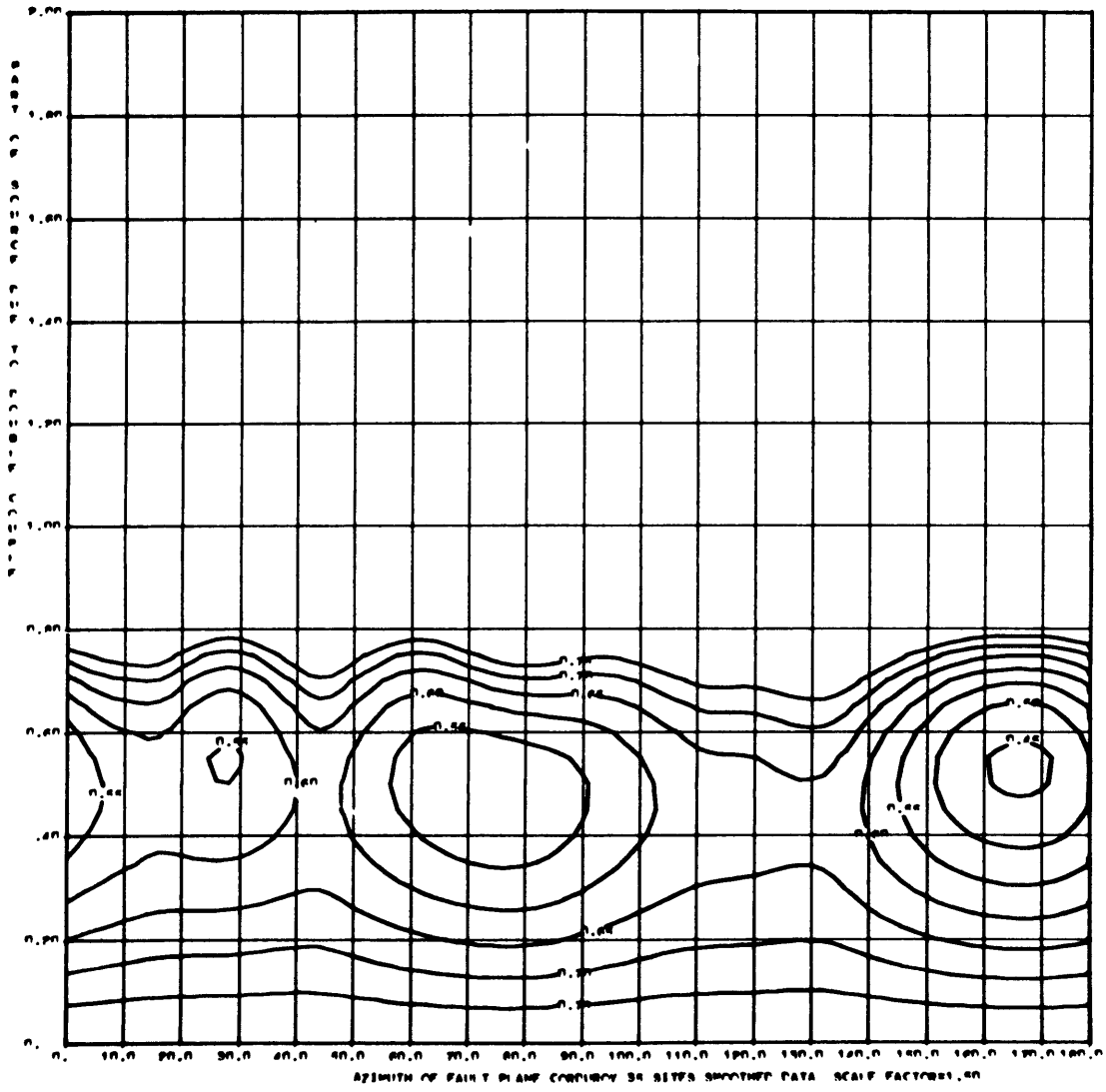

Fig. 31. S = 2.0

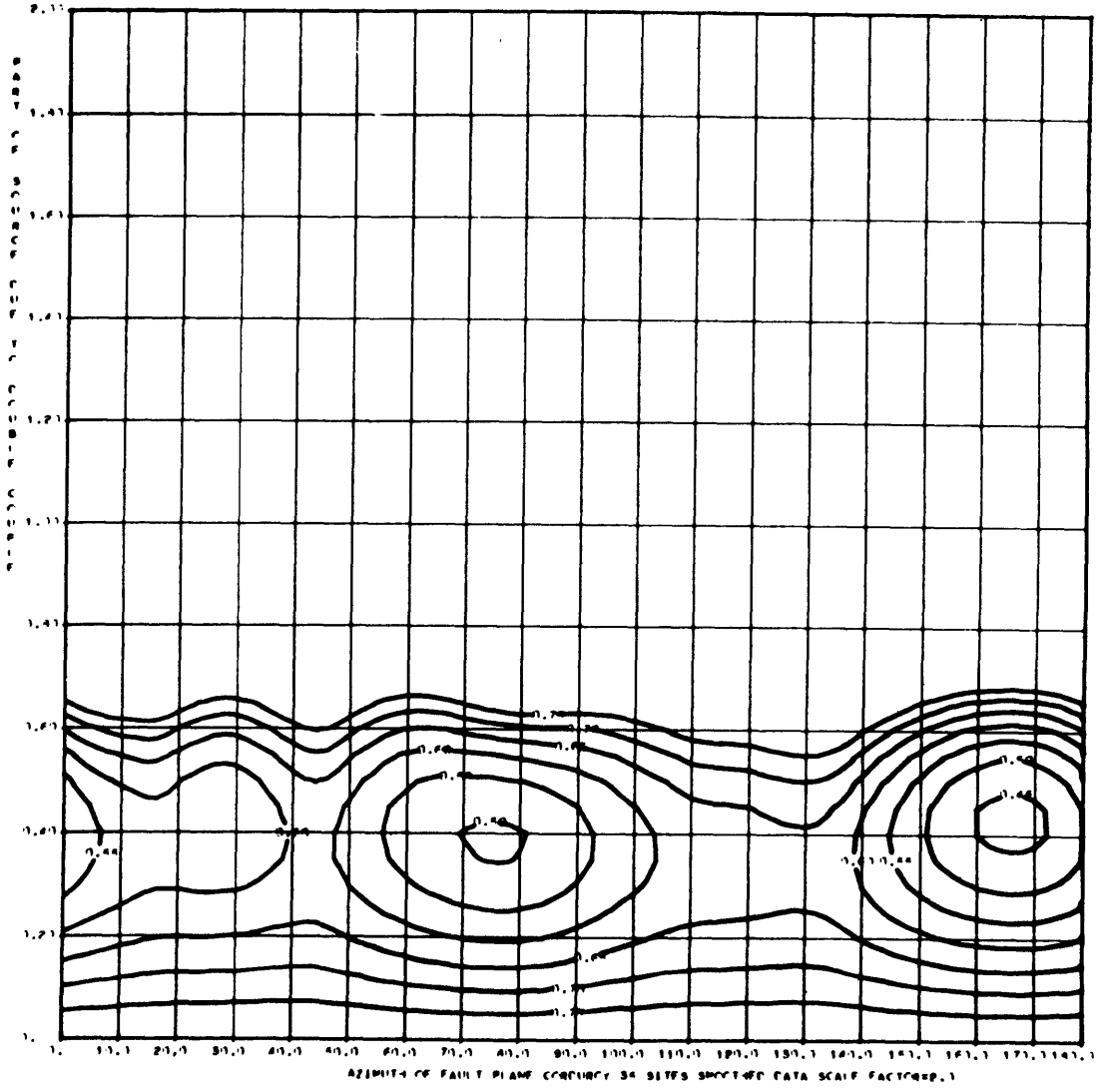
0.44
0.44
0.44
0.44
AZIMUTH OF FAULT PLANE CORRESPONDING TO BEST SPECTRAL DATA SCALE FACTOR

Fig. 32. Generalized geologic map of the Nevada Test Site with the location of explosions in relation to major faults. (Healey, 1968; Hoover, 1968)

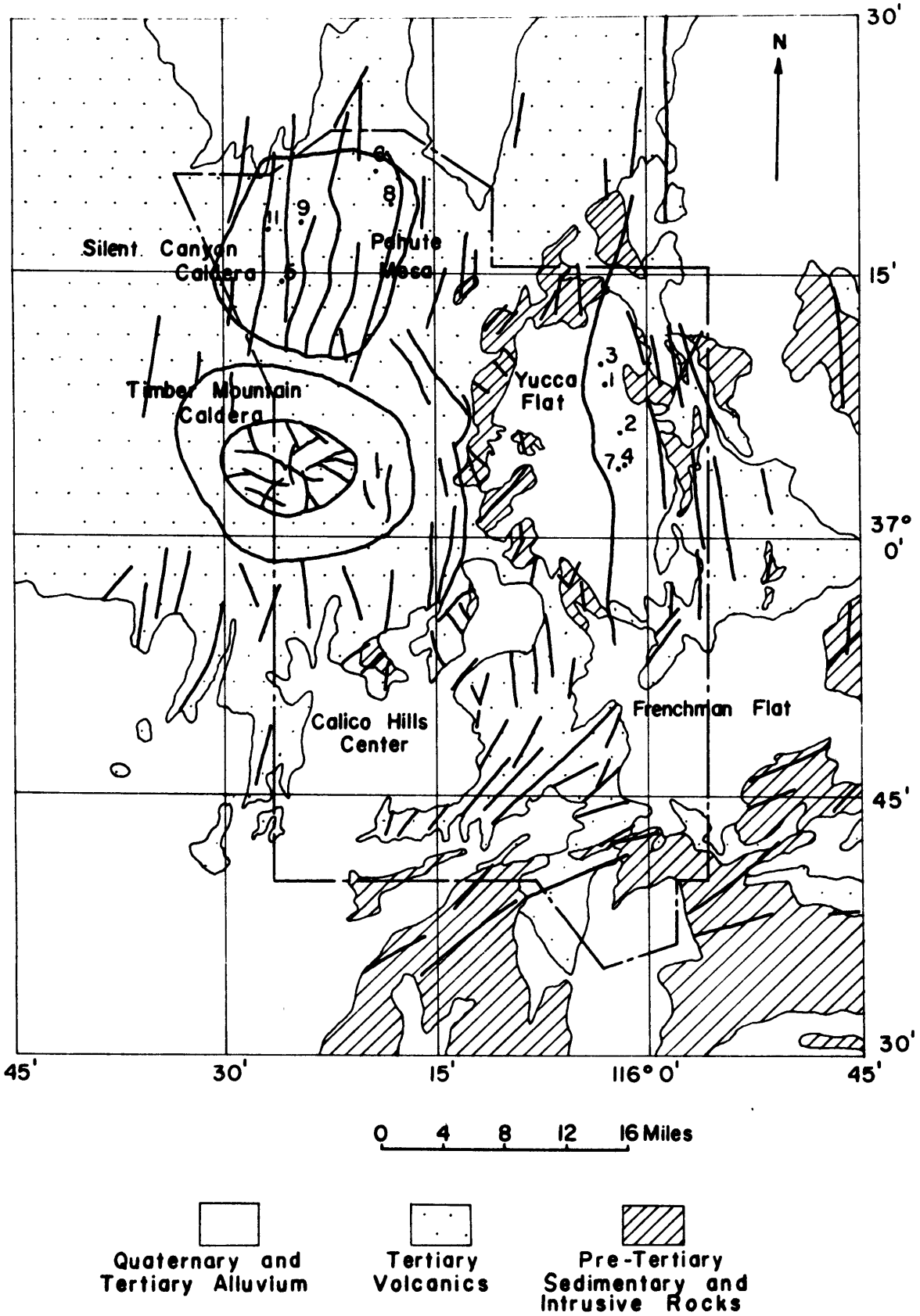
30'
N
15'
37° 0'
45'
30'
15'
116° 0'
45'
30'
Silent Canyon Caldera
Pahute Mesa
Timber Mountain Caldera
Yucca Flat
Calico Hills Center
Frenchman Flat
11
9
8
6
5
.3
.1
.2
7.4
0 4 8 12 16 Miles
Quaternary and Tertiary Alluvium
Tertiary Volcanics
Pre-Tertiary Sedimentary and Intrusive Rocks

Fig. 33. Yucca Flat with the fault plane solutions of three explosions in relation to the natural and explosion produced fracture trends. (Barosh, 1968)

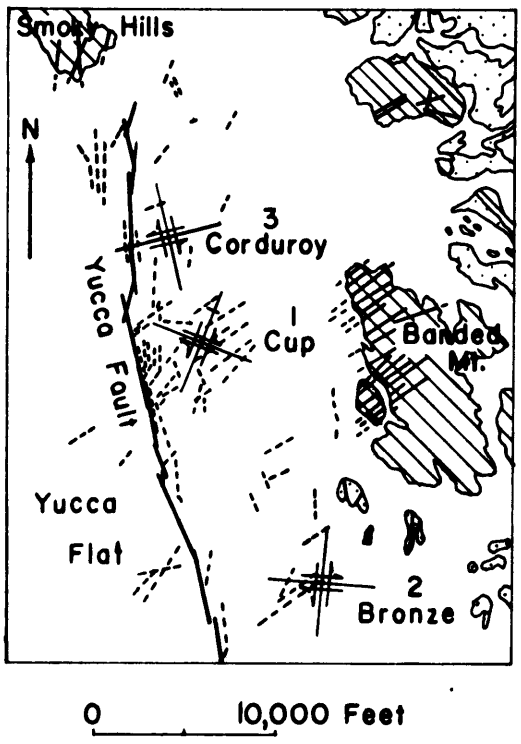
Smoky Hills
N
3
Corduroy
Yucca Fault
1
Cup
Banded Mt.
Yucca
Flat
2
Bronze
0
10,000 Feet
Alluvium
Volcanic Rocks
Sedimentary Rocks
Joint Trends in Bedrock
Explosion Produced Fracture Trends in Alluvium